

Electrochemical investigation of novel reference electrode Ni/Ni(OH)₂ in comparison with silver and platinum inert quasi-reference electrodes for electrolysis in eutectic molten hydroxide

Al-Shara, N. K., Sher, F., Yaqoob, A. & Chen, G. Z.

Author post-print (accepted) deposited by Coventry University's Repository

Original citation & hyperlink:

Al-Shara, NK, Sher, F, Yaqoob, A & Chen, GZ 2019, 'Electrochemical investigation of novel reference electrode Ni/Ni(OH)₂ in comparison with silver and platinum inert quasi-reference electrodes for electrolysis in eutectic molten hydroxide' International Journal of Hydrogen Energy, vol. 44, no. 50, pp. 27224-27236.

<https://dx.doi.org/10.1016/j.ijhydene.2019.08.248>

DOI 10.1016/j.ijhydene.2019.08.248

ISSN 0360-3199

Publisher: Elsevier

NOTICE: this is the author's version of a work that was accepted for publication in International Journal of Hydrogen Energy. Changes resulting from the publishing process, such as peer review, editing, corrections, structural formatting, and other quality control mechanisms may not be reflected in this document. Changes may have been made to this work since it was submitted for publication. A definitive version was subsequently published in International Journal of Hydrogen Energy, 44: 50, (2019) DOI: 10.1016/j.ijhydene.2019.08.248

© 2019, Elsevier. Licensed under the Creative Commons Attribution-NonCommercial-NoDerivatives 4.0 International <http://creativecommons.org/licenses/by-nc-nd/4.0/>

Copyright © and Moral Rights are retained by the author(s) and/ or other copyright owners. A copy can be downloaded for personal non-commercial research or study, without prior permission or charge. This item cannot be reproduced or quoted extensively from without first obtaining permission in writing from the copyright holder(s). The content must not be changed in any way or sold commercially in any format or medium without the formal permission of the copyright holders.

This document is the author's post-print version, incorporating any revisions agreed during the peer-review process. Some differences between the published version and this version may remain and you are advised to consult the published version if you wish to cite from it.

1 **Electrochemical investigation of novel reference electrode Ni/Ni(OH)₂ in**
2 **comparison with silver and platinum inert quasi-reference electrodes for**
3 **electrolysis in eutectic molten hydroxide**
4

5 Nawar K. Al-Shara^a, Farooq Sher^{b,*}, Aqsa Yaqoob^{a,c}, George Z. Chen^a

6 *a. Department of Chemical and Environmental Engineering, University of Nottingham, University*
7 *Park, Nottingham NG7 2RD, UK*

8 *b. School of Mechanical, Aerospace and Automotive Engineering, Faculty of Engineering,*
9 *Environmental and Computing, Coventry University, Coventry CV1 2JH, UK*

10 *c. Department of Chemistry, University of Agriculture, Faisalabad 38000, Pakistan*
11

12 **Abstract**

13 An efficient and green energy carrier hydrogen (H₂) generation via water splitting reaction has
14 become a major area of focus to meet the demand of clean and sustainable energy sources. In this
15 research, the splitting steam via eutectic molten hydroxide (NaOH-KOH; 49–51 mol%) electrolysis
16 for hydrogen gas production has been electrochemically investigated at 250–300 °C. Three types
17 of reference electrodes such as a high-temperature mullite membrane Ni/Ni(OH)₂, quasi-silver and
18 quasi-platinum types were used. The primary purpose of this electrode investigation was to find a
19 suitable, stable, reproducible and reusable reference electrode in a molten hydroxide electrolyte.
20 Cyclic voltammetry was performed to examine the effect on reaction kinetics and stability to
21 control the working electrode at different scan rate and molten salt temperature. The effect of
22 introducing water to the eutectic molten hydroxide via the Ar gas stream was also investigated.
23 When the potential scan rate was changed from 50 to 150 mV s⁻¹, the reduction current for the

* Corresponding author. Tel.: +44 (0) 24 7765 7754
E-mail address: Farooq.Sher@coventry.ac.uk (F. Sher)

24 platinum wire working electrode was not changed with newly prepared nickel reference electrode
25 that designates its stability and reproducibility. Furthermore, increasing the operating temperature
26 of molten hydroxides from 250 to 300 °C the reduction potential of the prepared nickel reference
27 electrode is slightly positive shifted about 0.02 V. This suggests that it has good stability with
28 temperature variations. The prepared nickel and Pt reference electrode exhibited stable and reliable
29 cyclic voltammetry results with and without the presence of steam in the eutectic molten hydroxide
30 while Ag reference electrode exposed positive shifts of up to 0.1V in the reduction potential. The
31 designed reference electrode had a more stable and effective performance towards controlling the
32 platinum working electrode as compared to the other quasi-reference electrodes. Consequently,
33 splitting steam via molten hydroxides for hydrogen has shown a promising alternative to current
34 technology for hydrogen production that can be used for thermal and electricity generation.

35
36 **Keywords:** Renewable energy; Hydrogen production; Eutectic molten hydroxide; Cyclo
37 voltammetry; Reference electrodes and Platinum working electrode.

38

39 **1 Introduction**

40 Hydrogen is an efficient energy carrier and emission free candidate to supersede the continuous
41 use of fossil fuels in future because of high mass energy density, fast kinetic rate of electrochemical
42 reaction and only water containing emission gas [1]. Hydrogen gas (H₂) can be produced from
43 biomass gasification, steam reformation of fossil fuel, coal gasification, partial oxidation of
44 hydrocarbons [2] and biomass fermentation [3]. All these resources have environmental issues
45 regarding CO₂ emission, global warming and greenhouse effect [4]. Most of the methods are not
46 green, therefore, electrolysis of water is one of the clean and renewable hydrogen production
47 method. This process has high end-product purity that can reach 99.9 vol% [5] and can be achieved

48 on both small and large-scale productions [6]. It is considered as promising recyclable green energy
49 carrier because of production of hydrogen without emission of CO₂ [7, 8] that can be used for
50 heating purposes, electricity production, as a fuel for running vehicles [9] and in the fabrication of
51 metal hydride batteries [10].

52
53 However, there are existing challenges and barriers in the production of hydrogen gas (H₂), storage
54 and safe transportation [11]. Splitting water is considered flexible, reliable, clean and sustainable
55 method that can produce hydrogen from water electrolysis, sunlight (photoelectrolysis), series of
56 exothermic and endothermic reactions (thermochemical electrolysis). Water electrolysis is
57 preferred over other techniques because yield and efficiency both are quite low for
58 photoelectrolysis and thermochemical electrolysis [12]. H₂ production via water electrolysis
59 included three methods: proton exchange membrane (PEM) electrolysis [13] solid oxide cell
60 electrolysis (SOCE) and alkaline electrolysis [14]. Hydrogen production via molten hydroxide
61 electrolysis is the most scalable technique and it has the main advantage that energy needed for
62 electrolysis is added as heat, which is cheaper than electricity [15]. In addition, this technique can
63 maintain the heat for electrolysis from current passing through electrolyte and the conductivity of
64 hydroxide electrolyte increased with increasing temperature or pressure. All this specification is
65 important for reaction kinetics, that reduced energy loss because of the electrode over potential and
66 increased the system efficiency [5].

67
68 The recent research focus is required to increase the efficiency of the electrolysis system and to
69 increase the rate of hydrogen gas production during high-temperature steam electrolysis [16].
70 However, the formation of hydrogen is influenced by the electrolyte type, concentration, electrode
71 properties, reaction temperature and pressure [17]. There are limited reference electrodes that have

72 been deemed suitable for a molten hydroxide. Miles et al. [18] explored electrochemically different
73 eutectic molten hydroxides (NaOH-KOH, LiOH-NaOH, LiOH-KOH) using palladium, nickel,
74 silver, aluminium, magnesium, zinc and Li-Fe working electrodes at 250–300 °C. They suggested
75 the use of Ag/AgCl as a reference electrode because of its faster reaction kinetics in molten
76 hydroxides. Ge et al. [19] investigated the nickel rod quasi-reference electrode for electro-
77 deoxidation of nickel oxide to prepare nickel powder in molten sodium hydroxide at 550 °C. They
78 were the first to conduct cyclic voltammetry on platinum as a working electrode using molten
79 NaOH at 550 °C.

80
81 The researchers used this material before investigating any other electrodes because of its relatively
82 high chemical stability. The anodic current was due to oxidation and increasing current at cathodic
83 limit can be attributed to the hydrogen evolution reaction. Guo et al. [2] presented the performance
84 and characterisation of a carbon fuel cell using molten hydroxides of NaOH at 550 °C and NaOH-
85 KOH (54:46 mol%) at 400 °C. Silver wire was used as a reference electrode in both cases. The
86 study found that the performance of the carbon fuel cell improved with a decrease in temperature
87 up to 400 °C using the eutectic mixture as an electrolyte. The CoP NA/CC electrocatalyst [20],
88 Pd₄Sn nanochain [21], PdCu clusters [22], PdCo nanodots [23], composite of γ -Fe₂O₃ [24] and 3D
89 macro porous foam of Ni, Cu and FeNi showed high catalytic activity for catalysing reaction at
90 electrodes surface. They exhibited excellent catalytic activity due to high surface area availability
91 and excellent mass transport to the electrode surface [25].

92
93 Yang et al. [26] also developed a direct ammonia fuel cell using a platinum electrode and a eutectic
94 electrolytic solution of NaOH-KOH (57–43 mol%). The cell was operated between 200 and 220
95 °C and achieved a maximum power of approximately 16 mW cm⁻². The cyclic voltammetry of the

96 platinum electrode was performed with a supply of argon gas or ammonia at 200 °C and Ag was
97 used as a reference electrode throughout the study. Litch et al. [1] found in their study that
98 increasing the temperature of molten NaOH or KOH beyond the maximum of 400°C decreased the
99 quantity of water available for hydrogen generation, instead of resulting in the formation of oxides.
100 This increase in temperature also decreased the coulombic efficiency of hydrogen gas. For the
101 combined hydroxide electrolyte (NaOH-KOH; 50–50 mol%), as temperature increased from 200
102 to 600 °C, the efficiency of hydrogen gas evolution decreased from 96% to 13.4%. This decrease
103 in hydrogen evolution was due to increment in parasitic side reaction (O^{2-} reduction) with a rise in
104 temperature that competes with hydrogen generation reaction.

105
106 Furthermore, Litch et al. [27] used eutectic molten hydroxide of NaOH-KOH at a 50:50 molar
107 ratio but only for the production of ammonia. They found that it was possible to produce ammonia
108 at an applied voltage of 1.2 V and at a coulombic efficiency of 35% alongside the excess
109 cogeneration of hydrogen. Moreover, the molten hydroxide was also used to develop a direct
110 carbon fuel cell at a low temperature. Hrnčiarikova et al. [28] studied the influence of the anode
111 composition: white cast iron (FeC), pure iron (Fe) and silicon-rich steel (FeSi) electrodes on the
112 electrochemical production of ferrate (VI) using molten KOH at temperatures of 110, 130 and 160
113 °C. The cyclic voltammetry indicated that the cathodic limit is represented by the evolution of the
114 hydrogen reaction. Subsequently, the anodic limit is represented by the evolution of the oxygen
115 reaction and the anodic peak is represented the melt decomposition. The development of these
116 peaks is dependent upon the operating temperature and the electrode materials used. There are
117 further studies on molten hydroxides that have used platinum wire [29] or copper plated platinum
118 [30] as a quasi-reference electrode respectively.

119

120 Zaafarany and Boller [31], investigated the behaviour of a copper electrode in 5 M of NaOH
121 solution electrochemically. The researchers found that the behaviour of the copper electrode in
122 NaOH solution was quite complicated. No simple relations were found between the voltage scan
123 rate and both peaks of current and of potential [31]. Xie et al., [32] explored the Ni₃N@Ni-Bi NS/Ti
124 as electrocatalyst for hydrogen production. It delivered the 10 mAcm⁻² of current density at 1.95 V
125 of cell potential by using benign condition and non-precious metal catalyst. The most popular
126 electrode material was found nickel as compared Co, Fe, or Cu due to its high catalytic activity,
127 more chemical stability, widespread availability as well as low cost [1].

128
129 Different reference electrodes such as Ag/AgCl at low temperature [33] mullite membrane-
130 enclosed Ag/AgCl [2], Graphite-protected silica tube Ag/AgCl [34] and alumina membrane tube
131 Ag/AgCl [35, 36] have been reported as options for high-temperature molten salt. All of these
132 previous studies have not been reported the use of a specifically fabricated reference electrode in
133 the eutectic molten hydroxide. Therefore, this research attempts to fill the gap in knowledge with
134 regards to finding suitable, stable and reusable reference electrodes for molten hydroxide system.
135 In addition, all of the studies reviewed above, an alkaline hydroxide salt was mainly used as an
136 electrolyte to construct the electrolysis cell and be used at both low and high temperatures. There
137 is no direct study as yet which focuses on developing steam electrolysis via eutectic molten
138 hydroxide for hydrogen production through the use of base metals. Therefore, this study mainly
139 contributes to filling this gap and working to increase the efficiency of hydrogen gas using base
140 metals in molten hydroxides.

141
142 Therefore, this study has focused on investigating the high-temperature mullite membrane
143 fabricated Ni/Ni(OH)₂, quasi-platinum, quasi-silver reference electrodes in eutectic molten

144 hydroxide. Furthermore, cyclic voltammetry was employed to scan and compare the electrode
145 potential stability and reliability of electrodes. The effect of introducing water to the eutectic
146 molten hydroxide via the Ar gas stream was investigated. This comparison is based on their effect
147 on the reaction kinetics and the stability to control the working electrode at the same operating
148 process conditions. Finding a reliable reference electrode will allow a proper understanding of
149 various working electrode materials that will be used in future. This can eventually lead to a further
150 increase in the electrode kinetics for increasing the hydrogen evolution reaction.

151

152 **2 Experimental**

153 In this study, various types of reference electrodes such as a high-temperature mullite membrane
154 Ni/Ni(OH)₂, quasi-silver and quasi-platinum types were used. The reason for using these different
155 types of reference electrodes was to find a suitable, stable, reproducible and reusable reference
156 electrode. The primary purpose of this electrode investigation is to understand the electrochemical
157 reactions involved during electrolysis in a molten hydroxide electrolyte. When the silver and
158 platinum quasi-reference electrodes were used in this study, these electrodes consisted simply of
159 metal wires with diameters of 1 mm and 0.5 mm respectively. The wires were individually attached
160 to a stainless steel rod 1.5 mm in diameter.

161 **2.1 Preparation of the Ni/Ni(OH)₂ reference electrode**

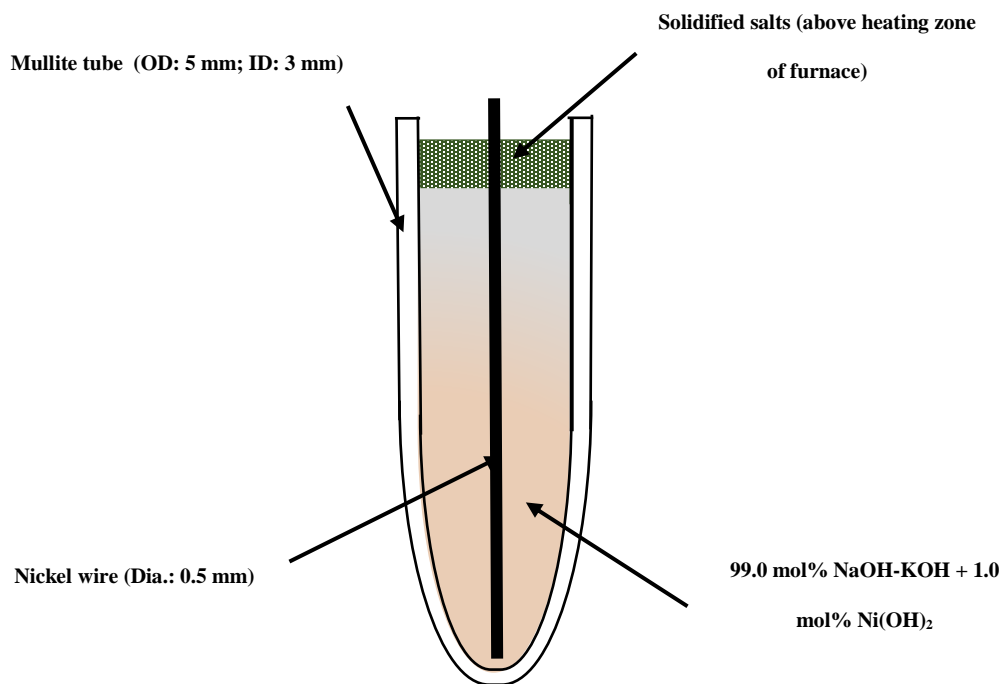
162 The mullite membrane was used to manufacture the reference electrode. The specifications of
163 commercial mullite tube were as 62% Al₂O₃, 36% SiO₂, 500 mm length, 5.0 mm diameter, and 1.0
164 mm thickness with a minimum bulk density of 2.7 g cm⁻³ with water absorption capacity of 0.02
165 vol% (Multi-Lab Ltd). 1 mol% Ni(OH)₂ (Arcos Organics) was mixed with the eutectic molten
166 hydroxide (NaOH-KOH; 49–51 mol%) (Internal electrolyte, Aldrich) and inserted into the tube

167 (mullite) forming the internal electrolyte of the reference electrode. Another key point to focus on
168 is the solubility of Ni(OH)₂ in molten hydroxides. It was reported by Gayer and Garrett [37] that
169 the solubility of Nickel hydroxide in an alkaline solution of NaOH at 25°C was low, while it was
170 high in any high acidic solution medium. Alternatively, the solubility product of Ni(OH)₂ of
171 6.5×10^{-18} was unchanged when observed from the reaction of nickel hydroxide with either base or
172 acid. A low concentration of 1.0 mol% of Ni(OH)₂ in this work was therefore used to make an
173 internal electrolyte mixture of the reference electrode”

174
175 The total amount of salt placed in the tube was 1.16 g. The tube was initially placed inside the retort
176 stand but once outside the crucible, it was filled quickly with the prepared mixture of salt to avoid
177 the hydroxides absorbing any moisture from the air. Note that the internal composition of eutectic
178 hydroxides is the same as that of the external electrolyte composition (i.e. the bulk electrolyte used
179 for electrolysis).

180
181 The temperature of the furnace was immediately raised above the working temperature of 300 °C
182 to completely melt the mixed salts in the tube [36]. It should be mentioned here that the mixture
183 was filled into the tube up to a length longer than the uniform heating zone (ca. 12 cm) of the
184 furnace. A nickel (Ni) wire (99.98% pure temper annealed, 0.5 mm diameter, Advent Ltd.) was
185 then inserted to the bottom of the tube containing the electrolyte mixture as the salt began to melt.
186 Subsequently, the tube was sealed and left for 24 h to complete the melting of the salt mixture.
187 Following this, the furnace was cooled to the working temperature so that the upper part of the
188 molten mixture in the tube solidified to seal the tube. Alkaline electrolysis prevents the catalyst
189 requirements and other issues of catalytic metals such as corrosion and ineffective cost. The
190 efficiency of electrolysis system has no need for precious catalytic metal and requires the use of

191 base metals instead to produce hydrogen gas [32]. This is because the molten hydroxide itself acts
192 as a catalyst during the process. Furthermore, the electrodes have to be resistant to corrosion, have
193 good electric connectivity, exhibit good catalytic properties and maintain a reliable structure during
194 the process [1, 38]. A schematic diagram of the Ni/Ni(OH)₂ reference electrode is shown in Fig.
195 1.



210 **Fig. 1.** A schematic of the Ni/Ni(OH)₂ reference electrode in a tube membrane.

211
212 Performance tests of the nickel reference electrode were conducted in a cylindrical alumina
213 crucible (>99%, 60 mm outer diameter, 120 mm height, 280 mL volume, Almath Crucibles Ltd.)
214 under an argon atmosphere, using an Ivium-Stat multichannel electrochemical analyser. In all of
215 the experiments, 250 g of the eutectic molten hydroxide (NaOH-KOH; 49–51 mol%) were left
216 under 40 cm³min⁻¹ of argon gas at 300 °C for 24 h before use.

217

218 **2.2 Experimental**

219 Three types of reference electrodes were used in this investigation. Silver wire (99.99% pure
220 temper annealed, 1.0 mm diameter, Advent Research Materials), and platinum wire (99.95% pure
221 temper annealed, 0.5 mm diameter, Advent Research Materials) as quasi-electrode and the mullite
222 membrane Ni/Ni(OH)₂ reference electrode. A platinum wire was used as the working electrode,
223 while a stainless steel rod (304 Grade, 5 mm diameter, Unicorn Metals) was used as the counter
224 electrode. In this study, stainless steel was chosen as the counter electrode material due to its
225 inherent stability and good electrical conductivity.

226

227 The performance tests were conducted in a cylindrical alumina crucible (>99 %, 60 mm of outer
228 diameter, 120 mm in height, 280 mL in volume, Almath Crucibles Ltd.) under an argon
229 atmosphere; using an Iviumn-Stat multichannel electrochemical analyser. In all experiments, 250
230 g of the eutectic hydroxide (NaOH-KOH; 49–51 mol%) was left under 40 cm³min⁻¹ of argon gas
231 at 300 °C for 24 h before beginning the electrochemical analysis. The furnace was then set to the
232 required experimental temperature.

233

234 Subsequently, the working temperature was reduced to the temperature that needs to be examined.
235 However, it was difficult to obtain the exact temperature for electrolyte because it can only be fixed
236 by changing the furnace set temperature. The furnace temperature controller in turn only has an
237 accuracy of ±1 °C. The electrolyte temperature was also influenced by additional factors such as
238 the effectiveness of the furnace insulation and the ambient temperature. These factors proved
239 difficult to maintain constant throughout all experiments. CV tests of nickel prepared reference

240 electrode showed the no change in reduction potential for the formation of NiO₂ at different scan
241 rate. CV tests were carried out using the same reference electrode for 10 days and were repeated
242 thrice. It was found that the lifetime of using the reference electrode is at least 7-9 days to avoid
243 any contamination of internal in the chosen eutectic molten hydroxide. Hence, the ideal ionic
244 membrane to use to construct a reference electrode for the eutectic molten hydroxide is mullite
245 because of its stability, reusability and longer lifetime. Cyclic voltammetry was employed to scan
246 and check the platinum working electrode potential stability and reliability with the three different
247 types of reference electrodes in the eutectic molten hydroxide.

248
249 The measurement was made using a platinum wire as a working electrode and one of the reference
250 electrodes (silver wire, platinum wire or the prepared nickel reference electrode). Platinum was
251 used as a working electrode with all reference electrodes before selecting any other working
252 electrode because of its relatively high chemical stability [19]. The immersion depth of the working
253 electrode was ~14 mm. During measurement, the scan started at an open circuit potential,
254 progressing in the negative direction before reversing in a positive direction. The scan rate was
255 varied during the tests and the effect of molten salt temperature was also considered. The steam
256 effect in eutectic molten hydroxide was also studied by cyclic voltammetry. The flow of the water
257 stream was maintained at 7.28 cm³min⁻¹ and it was mixed with argon gas at 40 cm³min⁻¹. This
258 steam and argon gas mixture were bubbled inside the eutectic molten hydroxide. Cyclic
259 voltammetry plots are expressed in current instead of current density because the platinum working
260 electrode was used at a fixed depth inside the eutectic molten hydroxide through this study [4].

261

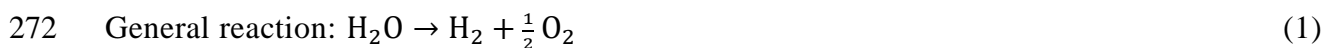
262

263

264 **3 Results and discussion**

265 **3.1 Standard reaction**

266 Before studying any electrochemical reaction in an alkali hydroxide with or without the presence
267 of water, it is imperative to study the possible reactions that can occur. Additionally, a calculation
268 of the standard reaction potential associated with these reactions must also be made. The possible
269 general reactions in an alkali hydroxide electrochemical process include H₂ and O₂ formation at the
270 cathode and anode respectively (reactions 1–3) [39]. The general reaction of an alkali hydroxide
271 which is in equilibrium with water and metal oxide is shown in reaction 4 [1].



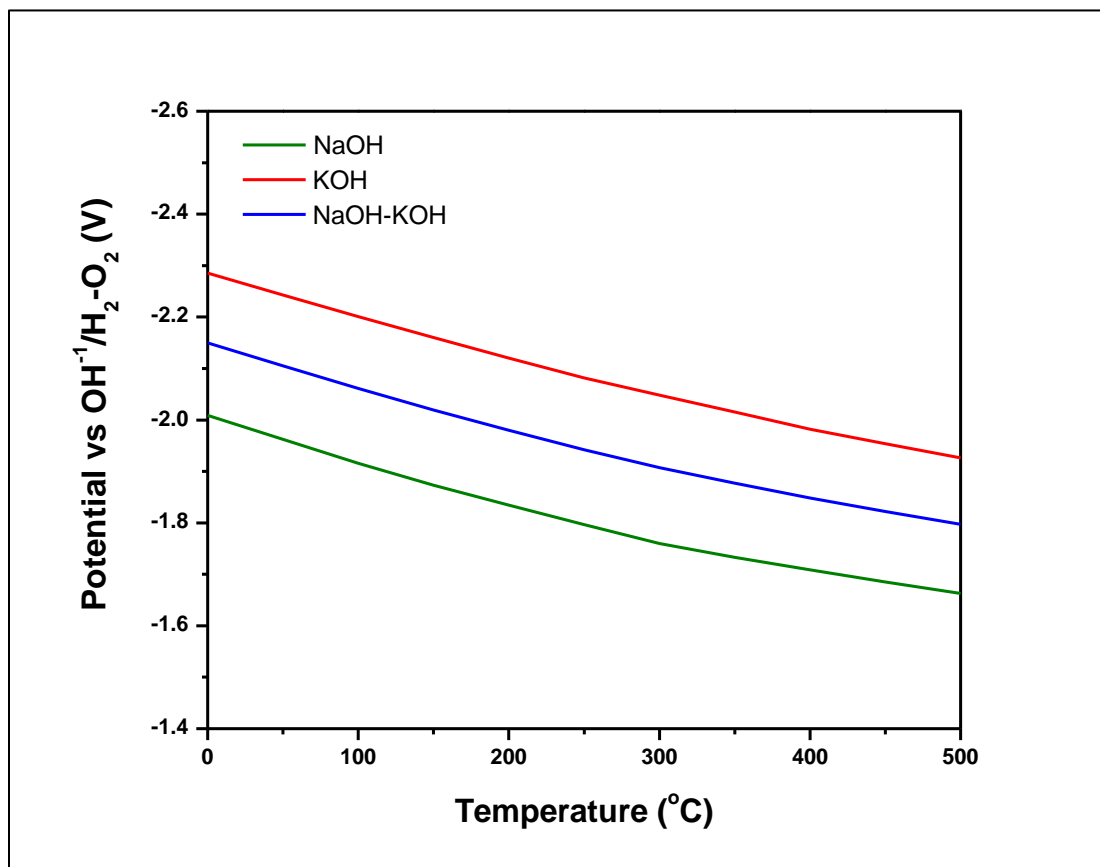
276
277 When the general reaction of water (1) is added to the reaction of hydroxide salt (4), the product
278 of this combination generates equivalent yields of hydrogen gas as in reaction (5):



280
281 From the reaction (5), it was clear that hydroxide salt was dehydrated and produced a metal oxide,
282 hydrogen and oxygen. For this reason, steam was continuously bubbled inside the eutectic molten
283 hydroxide in order to maintain equilibration hydration of molten hydroxide as steam splitting
284 occurs [1]. The corresponding standard reaction potential of reaction (4) was calculated using HSC

285 chemistry software (version 6.1; outotec) for the dissociation of the alkali hydroxide NaOH, KOH
286 and the eutectic mixture (NaOH-KOH; 49–51 mol%) as a function of temperature. This is shown
287 in Fig. 2.

288



289

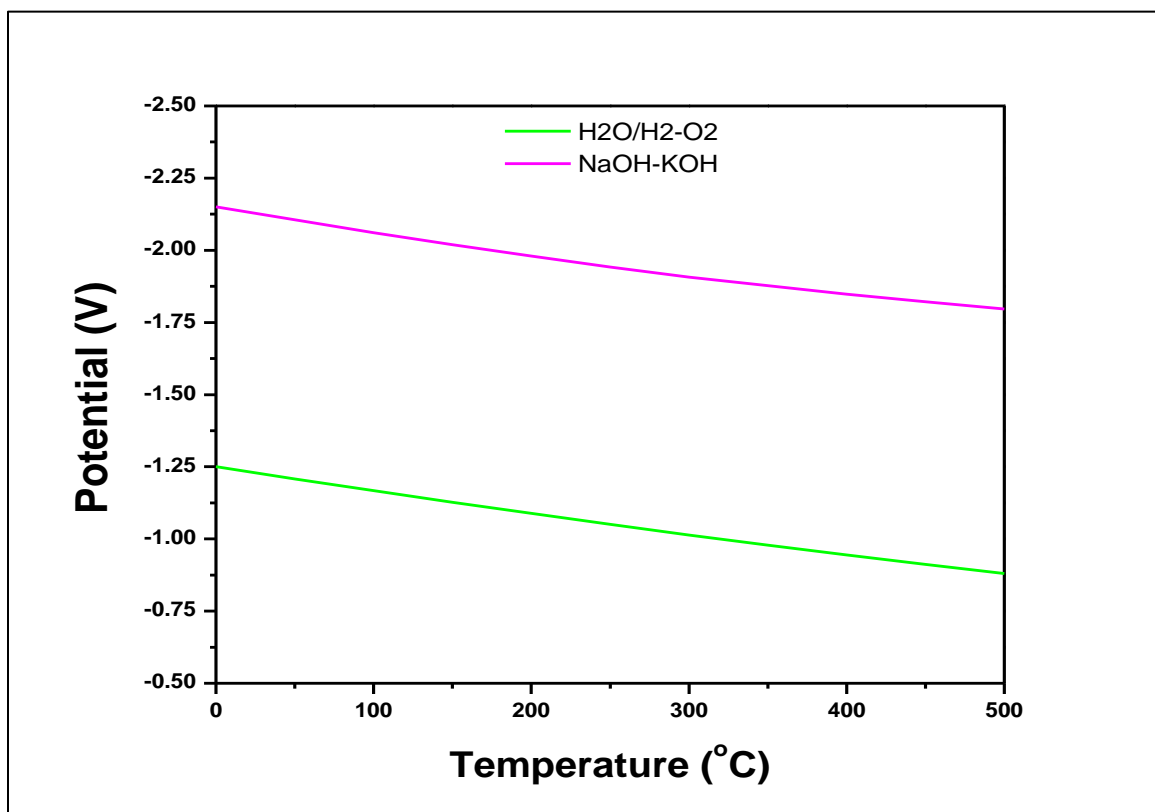
290 **Fig. 2.** Standard potential against temperature for the decomposition of molten hydroxides NaOH and KOH;
291 and the eutectic molten hydroxide (NaOH-KOH; 49–51 mol%) into their metal oxides (Na₂O and K₂O),
292 hydrogen gas (H₂) and oxygen gas (O₂). The potential was calculated using HSC chemistry software (version
293 6.1; outotec) and is reported versus the OH⁻/H₂-O₂ reference reaction.

294

295 It is obvious from Fig. 2 that the standard reaction potential required for splitting an alkali
296 hydroxide decreases with increasing temperature. In addition, the standard reaction potential for
297 reaction (1) (splitting H₂O to H₂ and O₂) is also calculated using the same software. Fig. 3 shows
298 the comparison between the standard reaction potential of reaction (1) and the standard reaction

299 potential of a binary mixture of hydroxides at a different temperature. This standard reaction
300 potential gives good information about the minimum energy required to carry out the reaction. The
301 standard potential for the formation of hydrogen gas as observed from Fig. 3 for the decomposition
302 of the eutectic molten hydroxide at 225 °C is -1.96 V. However, it is -1.06 V from splitting water
303 at the same temperature as shown in Fig. 3.

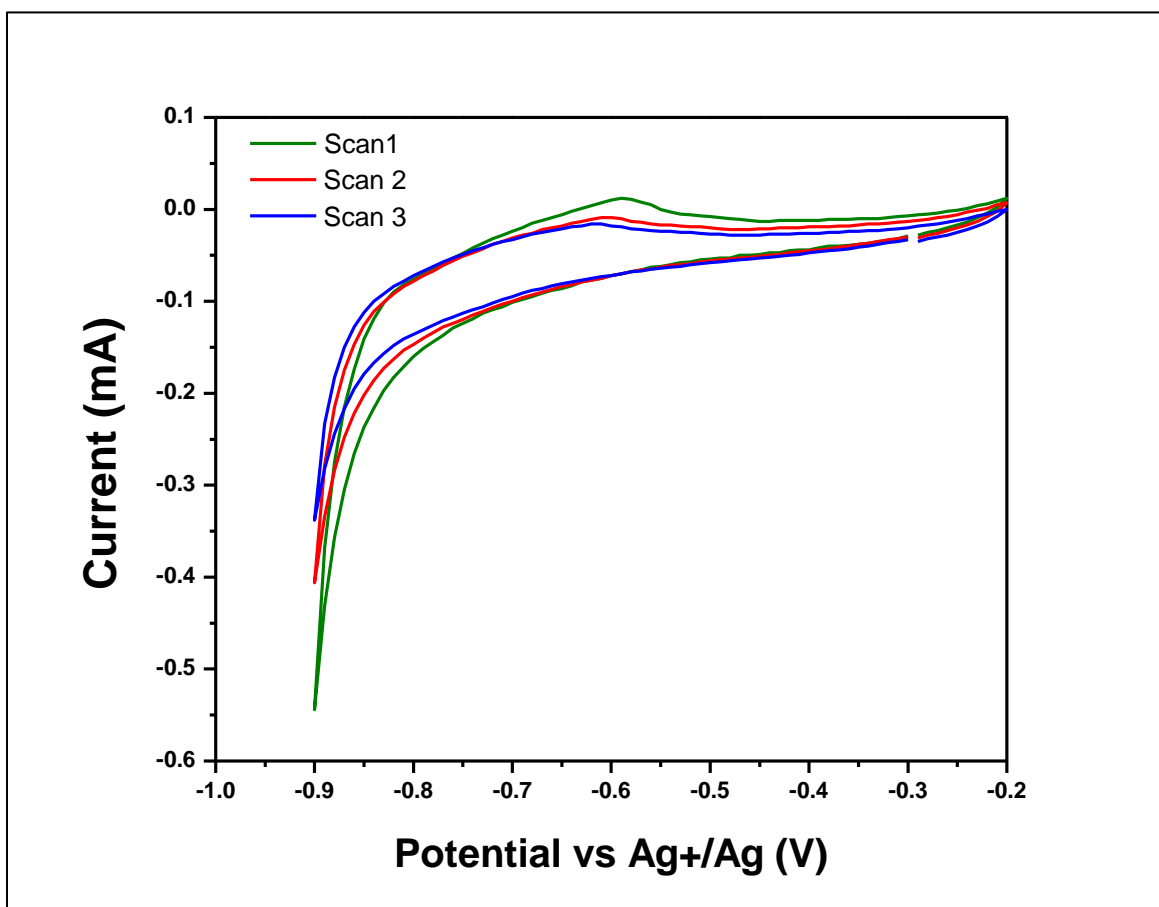
304



305
306 **Fig. 3.** Comparison between the standard potential of the splitting water (H₂O) into Hydrogen gas (H₂) and
307 oxygen gas (O₂) using the standard potential of decomposition of the eutectic molten hydroxide to their
308 metal oxide (Na₂O and K₂O), hydrogen gas (H₂) and Oxygen gas (O₂) respectively. The potential is
309 calculated using HSC chemistry software (version 6.1; outotec).
310

311 **3.2 Performance tests of Ag, Pt, and Ni/Ni(OH)₂ reference electrodes by cyclic**
312 **voltammetry**

313 The aim of this electrode investigation was to explore a suitable, stable, reproducible and reusable
314 reference electrode. Different scans were performed only to check the reproducibility and stability
315 of electrodes at same process conditions. Cyclic voltammetry of a platinum working electrode in
316 the eutectic molten hydroxide at 225 °C was carried out. The first examination used a silver wire
317 as the quasi-reference electrode. Fig. 4 shows the cyclic voltammetry data obtained at a scan rate
318 of 100 mV s⁻¹.



319
320 **Fig. 4.** Cyclic voltammograms of a 0.5 mm Pt wire in the eutectic molten hydroxide; scan rate: 100 mV s⁻¹;
321 ¹; CE: 5mm diameter stainless steel rod; an Ar gas atmosphere: 40 cm³min⁻¹. For negative scan limits of -
322 0.9 V RE: 1.0 mm Ag wire; immersion depth: 14 mm.
323

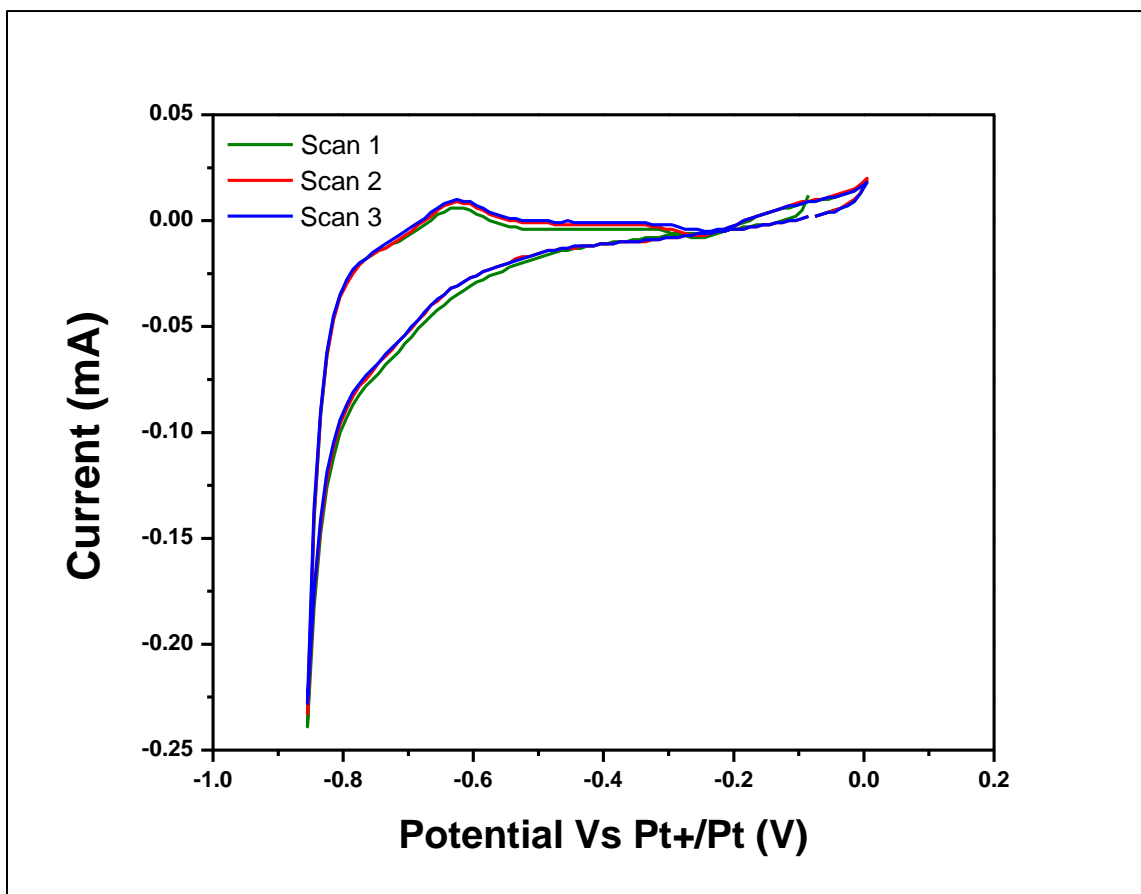
324 In Fig. 4, the potential range for cyclic voltammetry scans in this section to test the platinum wire
325 working electrode is set from -0.9 to -0.2 V against the silver reference electrode. Miles et al. [18]
326 reported that the reduction of water at the cathodic limit was -1.3 V vs a silver reference electrode.



328
329 Yang et al. [26] however, determined that the cathodic limit was -0.9 V vs a silver reference
330 electrode for a setup similar to this study. Therefore, the lower potential limit of -0.9 V vs Ag in
331 this study was used to avoid the negative influence of coexistent hydrogen gas. At the beginning
332 of the forward scan from -0.9 V vs Ag, the reduction current begins at a potential lower than -0.83
333 V and the current lesser than -0.5 mA. The potential window is kept between -0.83 and -0.2 V
334 which is roughly 0.6 V. Fig. 5 shows the preformed cyclic voltammetry of the platinum working
335 electrode in the eutectic molten hydroxide using a platinum quasi-reference electrode at a
336 temperature of 225 °C and a scan rate of 100 mV s⁻¹. CV is scanned negatively from -0.85 to 0.0 V
337 as presented in Fig. 5. The cathodic limit reaction from the above figure is influenced by reaction
338 (6) showing water decomposition ($2\text{H}_2\text{O} + 2\text{e}^- \rightarrow \text{H}_2 + 2\text{OH}^-$). This water is already formed at the
339 anodic limits as reported by Hives et al. [29] who found that the reduction potential limit was about
340 -0.81 V vs Pt. This is in agreement with findings observed from Fig. 5 which exhibit a value of -
341 0.8 V. The potential window of the general reaction (5) ranges between -0.83 and -0.025 V, which
342 is approximately 0.8 V. A prepared nickel reference electrode was also used during the CV
343 investigation on a platinum working electrode at a temperature of 225 °C and a scan rate of 100
344 mV s⁻¹. The CV results obtained are displayed in Fig. 6.

345

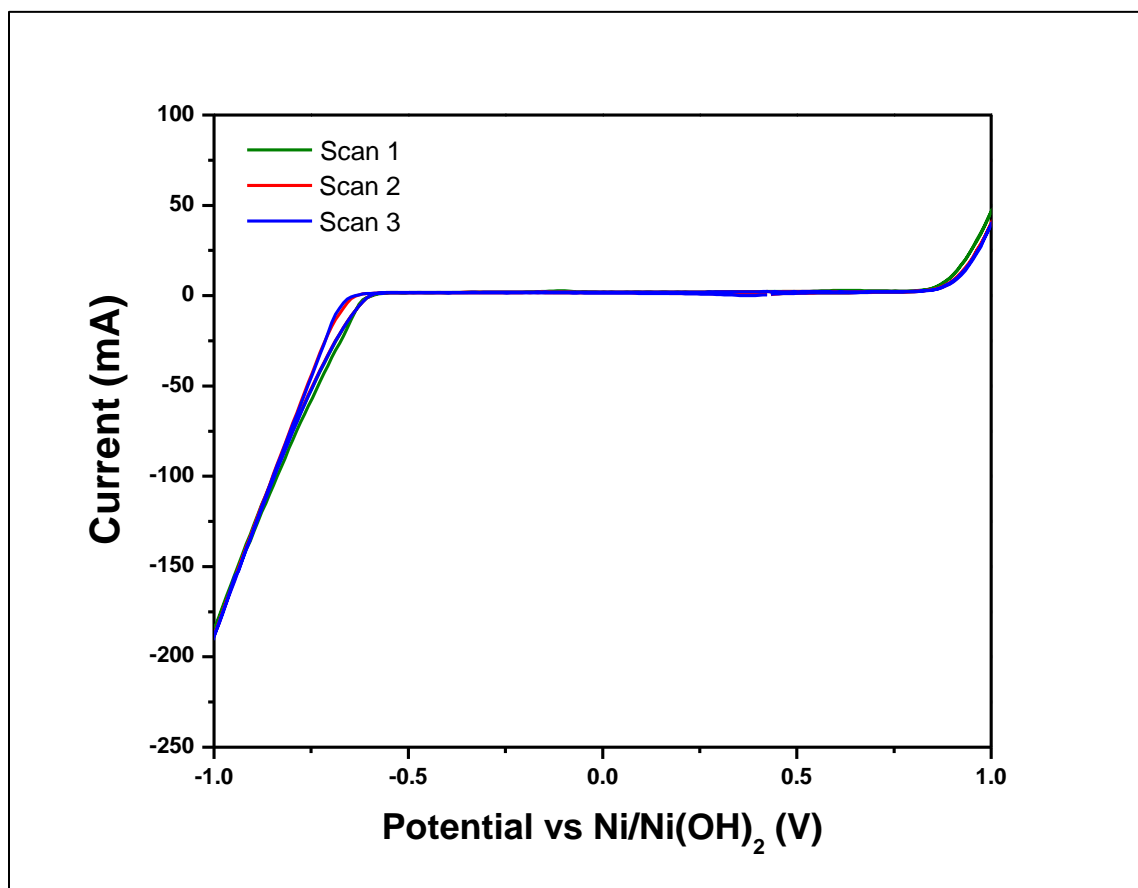
346



347
 348 **Fig. 5.** Cyclic voltammograms of a 0.5 mm Pt wire in the eutectic molten hydroxide; scan rate: 100 mV s^{-1} ;
 349 CE: 5mm diameter stainless steel rod; an Ar gas atmosphere: $40 \text{ cm}^3\text{min}^{-1}$. For negative scan limits of -
 350 0.85 V RE: 0.5 mm Pt wire; immersion depth: 14 mm.
 351

352 In Fig. 6, cyclic voltammetry CV is scanned negatively from -1.0 to 1.0 V vs Ni/Ni(OH)₂. The
 353 potential for water reduction to hydrogen gas is initiated at -0.69 V versus Ni/Ni(OH)₂. This water
 354 originates from the oxidation of hydroxide ions at the anodic limits as expressed in ($2\text{OH}^- \rightarrow$
 355 $\frac{1}{2}\text{O}_2 + \text{H}_2\text{O} + 2\text{e}^-$) of reaction (3). The electro-stability window of reaction (5)
 356 ($2\text{MOH} \rightarrow \text{H}_2 + \frac{1}{2}\text{O}_2 + \text{M}_2\text{O}$) is 1.68 V. This result somewhat agrees with the findings in terms of
 357 electro stability windows. In the case of the authors, this was reported to be about 1.4 V even
 358 though the reduction and the oxidation potential were different from the current study. This
 359 difference in the potential can be attributed to a variation in the reference electrode used. Ge et al.

360 [6] used a nickel rod as a quasi-reference electrode while this study used a prepared mullite
361 membrane Ni/Ni(OH)₂ reference electrode to control the working electrode potential.
362



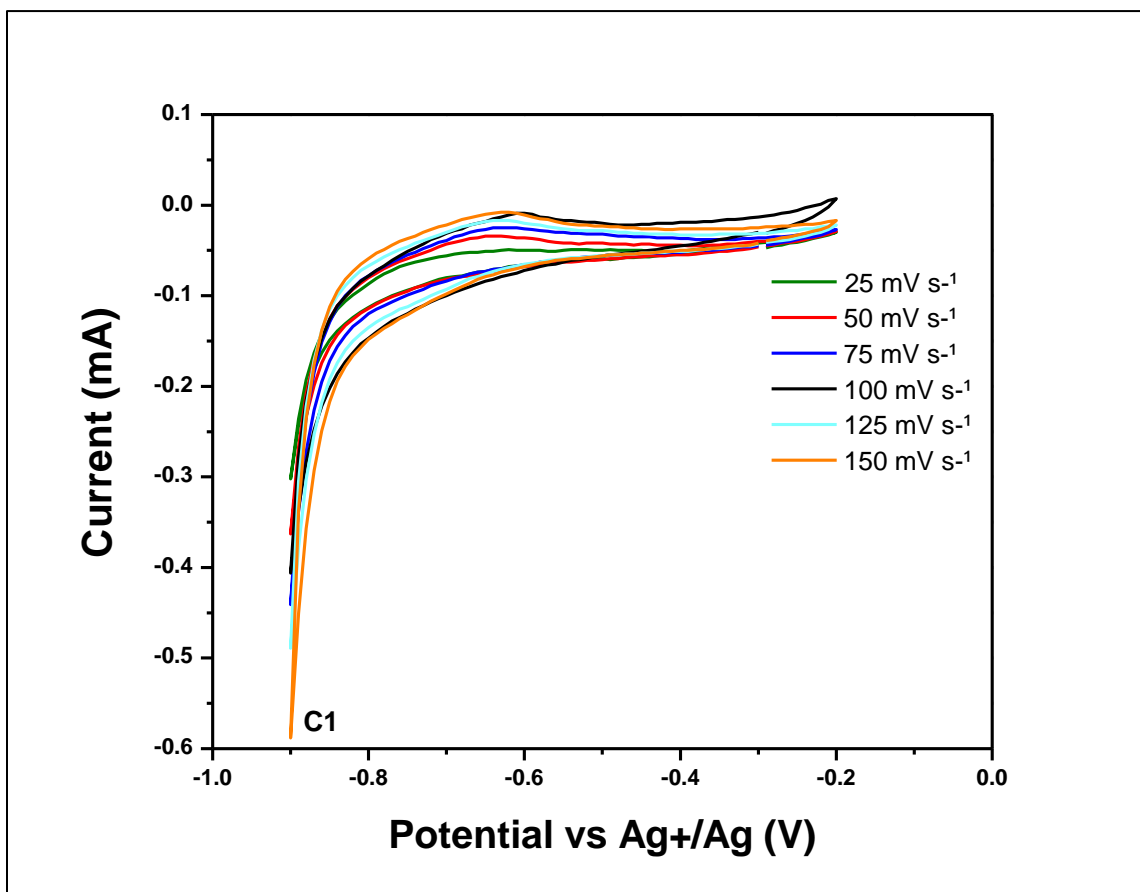
363
364 **Fig. 6.** Cyclic voltammograms of a 0.5 mm Pt wire in the eutectic molten hydroxide; scan rate: 100
365 mV s⁻¹; CE: 5 mm diameter stainless steel rod; an Ar gas atmosphere: 40 cm³min⁻¹. For negative
366 scan limits of -1.0 V Ni/Ni(OH)₂ in a mullite tube; immersion depth: 14 mm
367

368 Fig. 4, Fig. 5 and Fig. 6 indicate the potential of working electrode irrespective of the reference
369 electrodes. No cathodic peak or oxidation peak is visible prior to the start of the current wave
370 around the cathodic and anodic limit respectively when the platinum wire was used as a working
371 electrode. This observation indicates that the platinum working electrode was inert in the eutectic
372 molten hydroxide at least within the relatively short experimental time scale considered in this

373 study. From Fig. 3, the general standard potential for the reduction of hydroxide ions to the
374 hydrogen gas, oxygen gas and oxides of the reaction (5) ($2\text{MOH} \rightarrow \text{H}_2 + \frac{1}{2} \text{O}_2 + \text{M}_2\text{O}$) is -1.96 V at
375 225 °C. This standard potential is close to -1.68 V vs Ni/Ni(OH)₂ as obtained from Fig. 6 which
376 confirm its stability and reproducibility. The comparison of cyclic voltammograms of each
377 reference electrode shows that the prepared nickel has more stability in comparison to silver and
378 platinum quasi-reference electrodes. The Ni₃N@Ni-Bi NS/Ti electrocatalyst reported by [32]
379 showed more stability and efficient catalytic activity for 20h. There was no variation in current
380 density after 1000 CV cycles that confirmed its stability as well as durability. Liu et al [40] reported
381 the Ni₃N NA/CC as an efficient electrocatalyst for hydrogen evolution because of durable and
382 excellent catalytic activity was observed for 8 hours. It produced 10 mA cm⁻² at 1.35 V potential
383 with 1.0 M KOH as well as 0.33 M urea. The nickel prepared reference electrode in the current
384 study has more stability as compared to the above previous studies that was observed for 24h.

385 **3.3 Effect of changing the potential scan rate**

386 Cyclic voltammetry investigations at different potential scan rates were carried out for the platinum
387 working electrode in the eutectic molten hydroxide. This investigation was also carried out using
388 the above-mentioned reference electrodes (silver and platinum quasi-reference electrode, and
389 Ni/Ni(OH)₂) to control the working electrode potential. Fig. 7 shows the obtained cyclic
390 voltammetry in the eutectic molten hydroxide at 225 °C and at the scan rates ranging between 25
391 and 150 mV s⁻¹. Silver wire was used as the reference electrode.



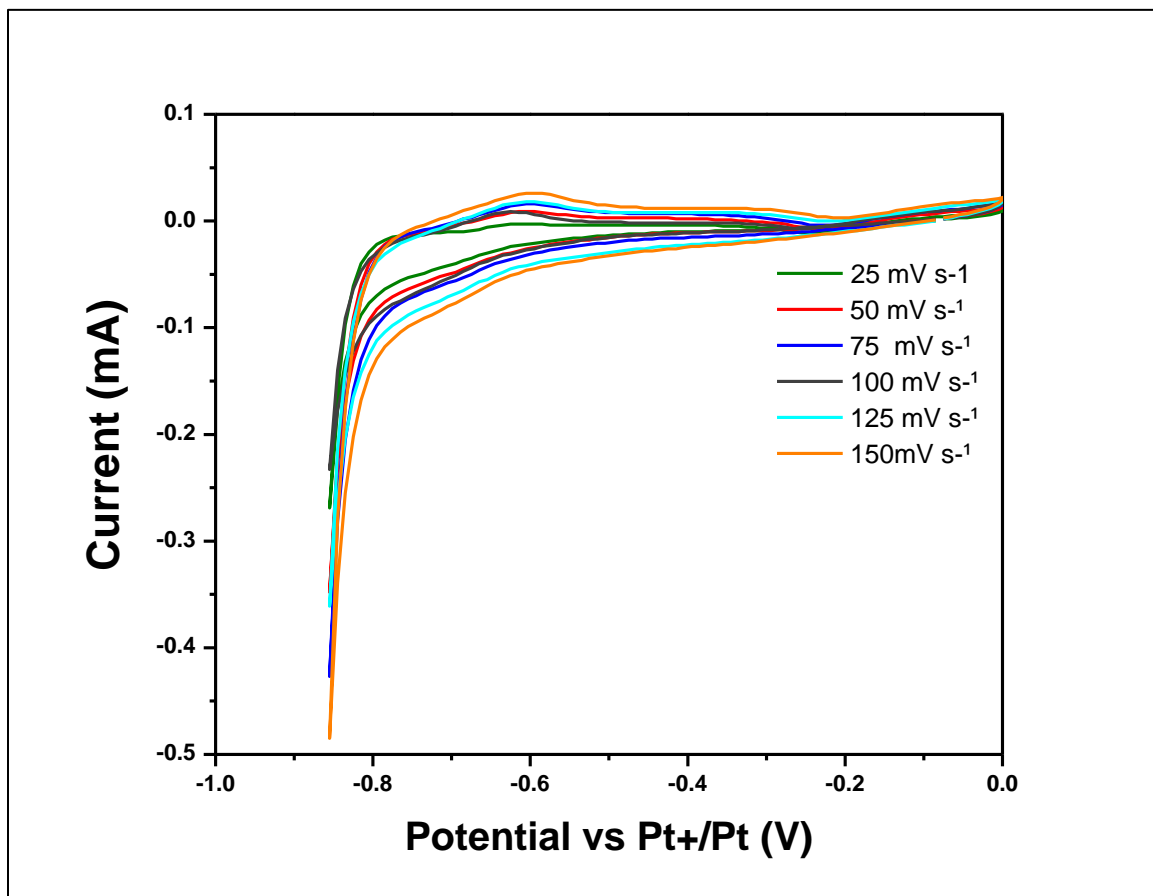
392
 393 **Fig. 7.** Cyclic voltammograms of a 0.5 mm Pt wire working electrode in the eutectic molten hydroxide at
 394 225 °C. For the indicated scan rates; CE: 5 mm diameter stainless steel rod; immersion depth: 14 mm; an
 395 Ar gas atmosphere: 40 cm³min⁻¹; for negative scan limit of -0.9 V, RE: 1.0 mm Ag wire.

396
 397 The height of the cathodic current at the reduction limit C1 increases with an increase in the speed
 398 of the potential scan rate as shown in Fig. 7. The various, recorded reduction currents are
 399 summarised in

400
 401 Table 1. Using these, obtained results showcase a relationship between the reduction current and
 402 the square root of the potential scan rate, demonstrating that mass transport can occur under semi-
 403 infinite linear diffusion conditions as in (7):

404
$$I_R = -0.0998 - 0.0347 v^{\frac{1}{2}} \quad (R^2 = 0.7849; \text{Ag wire}) \quad (7)$$

405
 406 Varying the rate at which the Pt working electrode was scanned using a Pt reference electrode,
 407 gave similar CVs in Fig. 8 as those obtained for Ag reference electrode.



408
 409 **Fig. 8.** Cyclic voltammograms of a 0.5 mm Pt wire working electrode in the eutectic molten hydroxide at
 410 225 °C. For the indicated scan rates; CE: 5 mm diameter stainless steel rod; immersion depth: 14 mm; an
 411 Ar gas atmosphere: 40 cm³min⁻¹; for negative scan limit of -0.85 V, RE: 0.5 mm Pt wire.

412
 413 The reduction current of the cathodic limit also increased with an increase in the speed of the scan
 414 rate. Equation (8) provides the linear relationship between the reduction current and the square root
 415 of the scan rate, demonstrating that mass transport can occur under semi-infinite diffusion
 416 conditions:

417
$$I_R = -0.1645 - 0.0211 \sqrt{v} \quad (R^2 = 0.677; \text{Pt wire}) \quad (8)$$

418 The prepared nickel reference electrode was also used to control the platinum working electrode at
 419 the same operating conditions. Hence its stability was compared with the silver and the platinum
 420 reference electrodes at different scan rates as shown in Fig. 9.

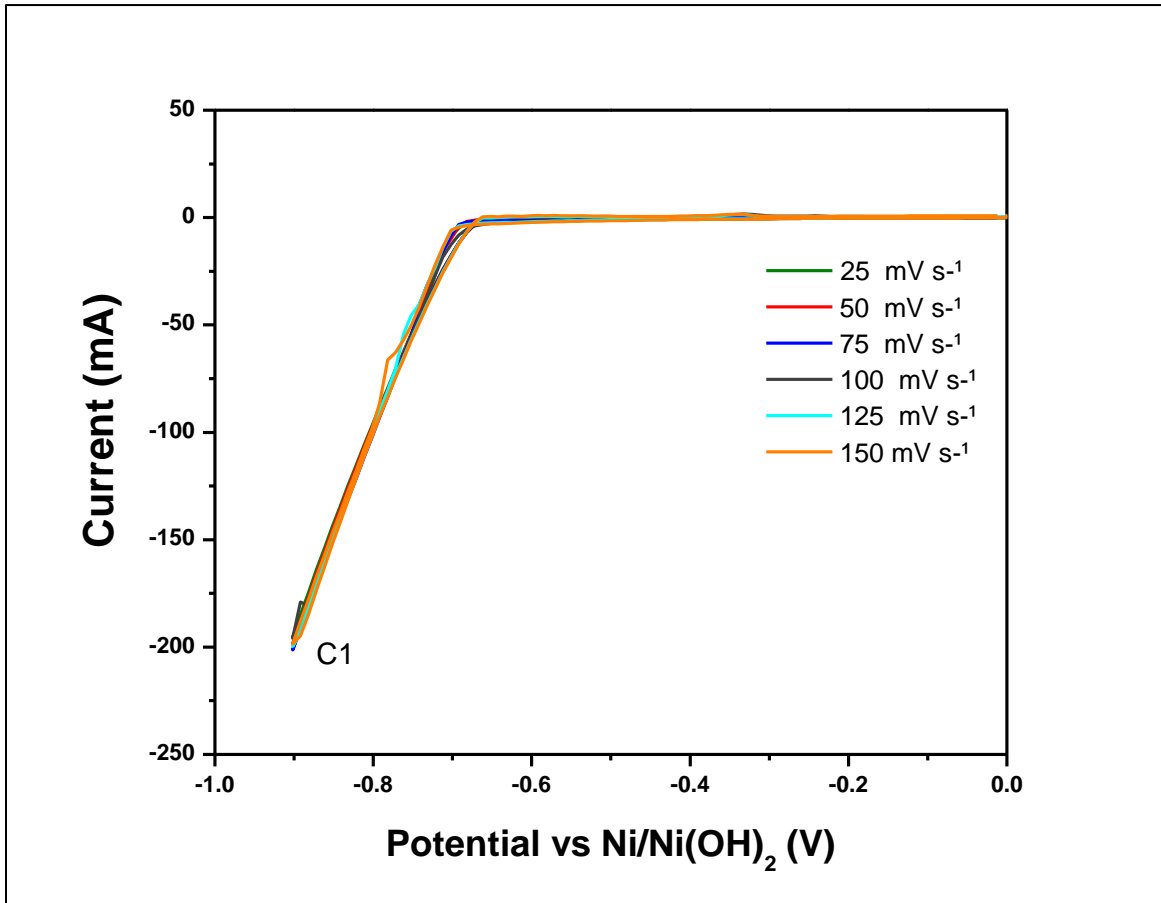
421
 422 **Table 1.** The current limits of a 0.5 mm Pt wire working electrode in the eutectic molten hydroxide at 225
 423 °C. For the indicated scan rates; CE: 5 mm diameter stainless steel rod; immersion depth: 14 mm; an Ar gas
 424 atmosphere: 40 cm³ min⁻¹.

Scan rate (mV s ⁻¹)	Ag wire	Pt wire	Ni/Ni(OH) ₂
	cathodic current limit (mA)	cathodic current limit (mA)	cathodic current limit (mA)
25	-0.31	-0.27	-197.50
50	-0.36	-0.34	-198.57
75	-0.33	-0.48	-199.39
100	-0.41	-0.23	-199.41
125	-0.48	-0.36	-199.66
150	-0.58	-0.48	-198.70

425

426

427



428
 429 **Fig. 9.** Cyclic voltammograms of a 0.5 mm Pt wire working electrode in the eutectic molten hydroxide at
 430 225 °C. For the indicated scan rates; CE: 5 mm diameter stainless steel rod; Immersion Depth: 14 mm; an
 431 Ar gas atmosphere: 40 cm³min⁻¹; for negative scan limit of -0.9 V RE: Ni/Ni(OH)₂ in a mullite tube.
 432

433 The comparison between the reference electrodes was based on checking the stability of the
 434 reduction current at different potential scan rates. It is obvious from Fig. 9 with the Ni/Ni(OH)₂
 435 reference electrode that the reduction current for the platinum wire working electrode at different
 436 scan rates did not change as the scan rate increased. Furthermore, it can be determined that the
 437 mass transport reaction between water and the electrode occurs under semi-infinite linear diffusion
 438 conditions as in equation (9):

439
$$I_R = -193.38 - 0.2992 v^{1/2} \left(R^2 = 0.8799; \frac{Ni}{Ni(OH)_2} \right) \quad (9)$$

440 In contrast, there is an increase noted in the reduction current as the scan rate increased when either
441 silver or platinum electrodes were used as a reference electrode as observed in Fig. 7 and Fig. 8.
442 However, the prepared nickel reference electrode showed stability in the reduction current and did
443 not show any change with increase the scan rate as shown in Fig. 9 This result further provides
444 evidence regarding the stability of the prepared nickel reference electrode. This stability and
445 reliability of a mullite membrane covering Ni/Ni(OH)₂ is attributed to the eutectic molten
446 hydroxide being able to penetrate through and react with the SiO₂; thus forming a stable ion channel
447 between the internal electrolyte (Ni(OH)₂-(NaOH-KOH)) and external electrolyte of the eutectic
448 molten hydroxide [41].

449

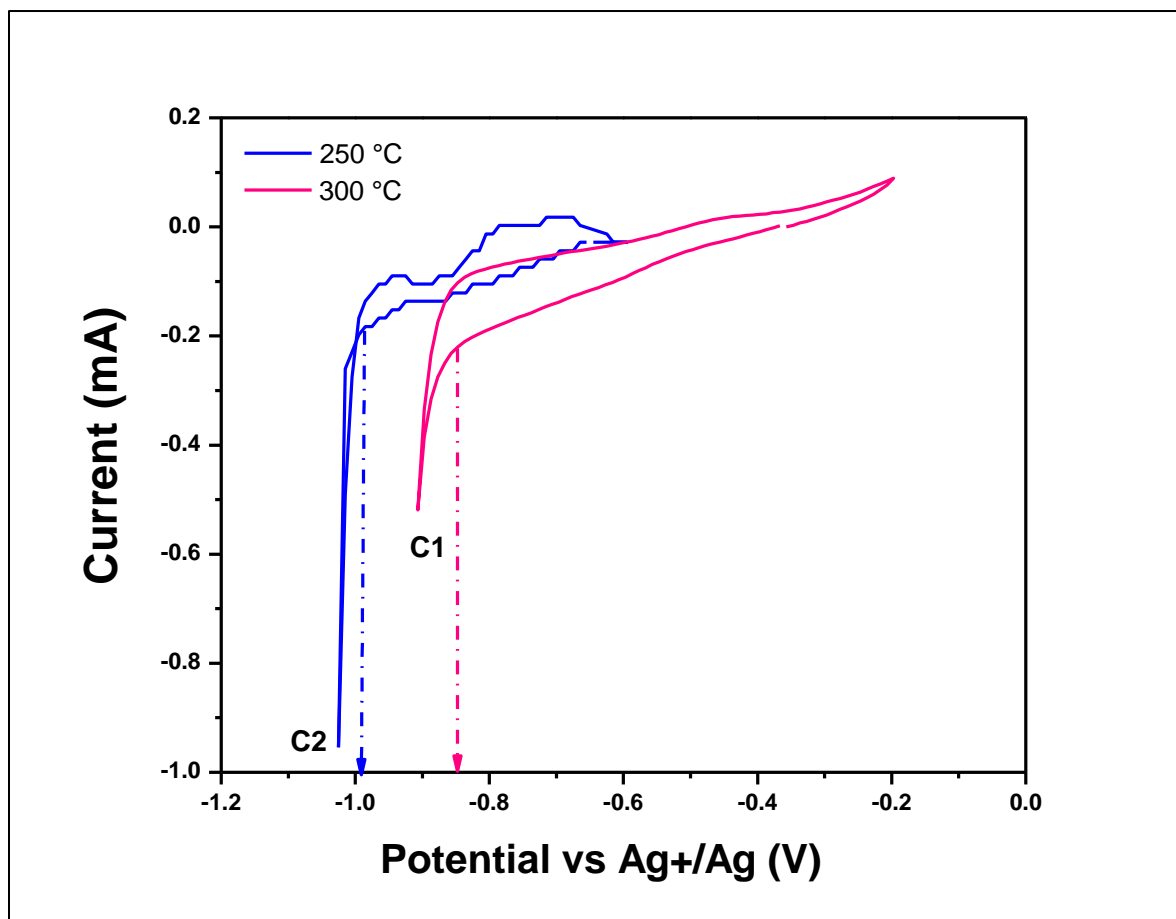
450 **3.4 Effect of changing the eutectic molten hydroxide operating temperature**

451 The effect of the eutectic molten hydroxide operating temperature on the cyclic voltammetry
452 studies and hence reference electrode stability was also investigated. A platinum wire was also
453 used as the working electrode in the eutectic molten hydroxide while the reference electrodes were
454 silver, platinum (both wires) and the mullite membrane Ni/Ni(OH)₂. Fig. 10 shows cyclic
455 voltammograms obtained at temperatures of 250 and 300 °C and a scan rate of 100 mV s⁻¹ using
456 silver wire as a reference electrode to control the working electrode potential.

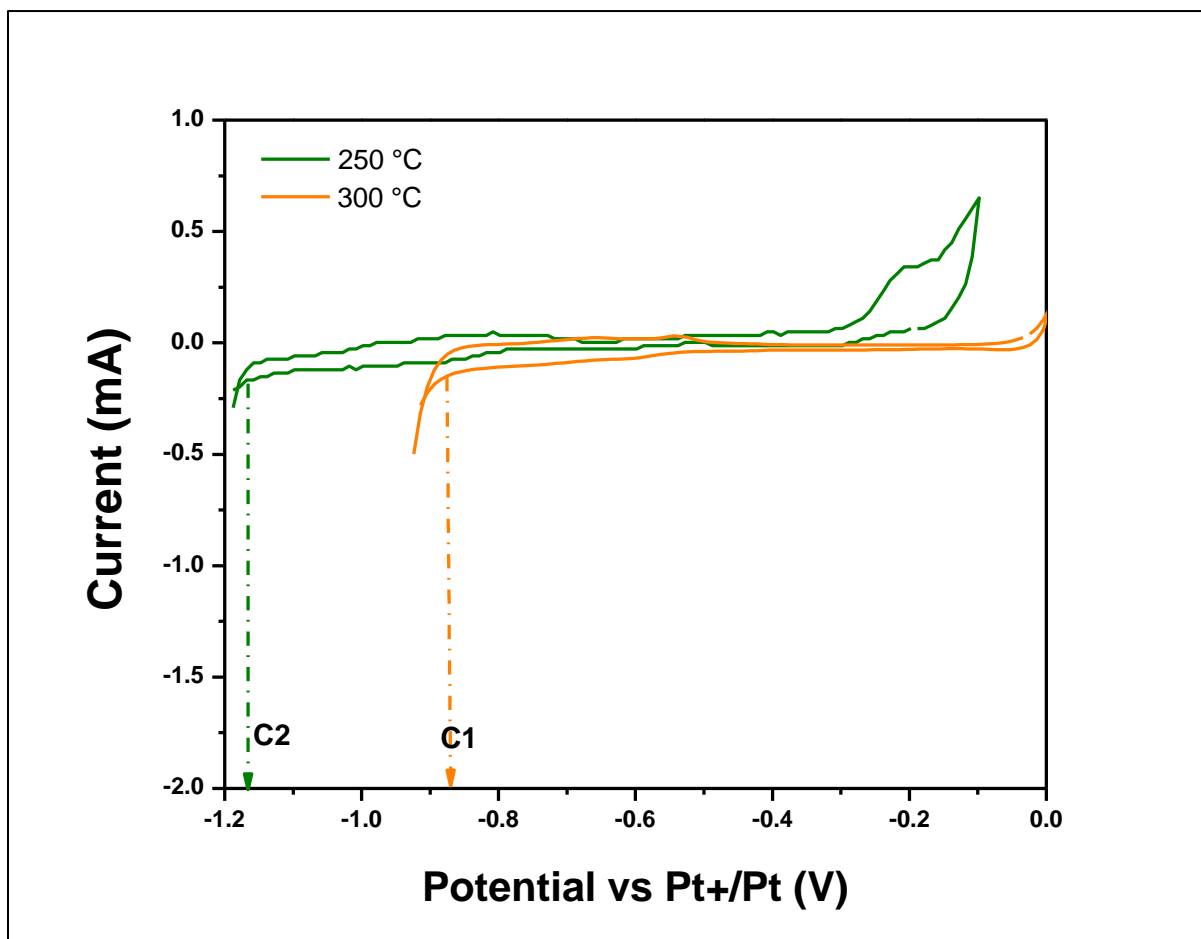
457

458 From the CVs displayed in Fig. 10, the cathodic limit shifts positively (~0.13 V) between (C2 and
459 C1) as the operating temperature of the eutectic molten hydroxide increases from 250 to 300 °C.
460 This positive increase in the reduction potential is due to the increase in the operating temperature
461 which in turn affects directly the electrode kinetics. A similar observation was obtained when the

462 platinum wire was used as the reference electrode as shown in Fig. 11. The recorded reduction
463 potentials for the reference electrodes used are tabulated in
464 Table 2. The results clearly indicate a positive shift in the working electrode potential with a molten
465 salt temperature variation of 50 °C for the Ag and Pt electrodes respectively.
466



467
468 **Fig. 10.** Cyclic voltammograms of a 0.5 mm Pt wire working electrode in the eutectic molten hydroxide at
469 different operating temperatures and a scan rate of 100 mV s⁻¹; CE: 5 mm diameter stainless steel rod;
470 immersion depth: 14 mm; an Ar gas atmosphere: 40 cm³min⁻¹. RE: 1.0 mm Ag wire.



471
 472 **Fig. 11.** Cyclic voltammograms of a 0.5 mm Pt wire working electrode in the eutectic molten hydroxide at
 473 different temperatures and a scan rate of 100 mV s^{-1} ; CE: 5 mm diameter stainless steel rod; immersion
 474 depth: 14 mm; an Ar gas atmosphere: $40 \text{ cm}^3\text{min}^{-1}$. RE: 0.5 mm Pt wire.
 475

476 In the case of the platinum reference electrode, a positive shift of 0.22 V is observed between (C2
 477 and C1) which is 0.1 V higher than when using the silver wire reference electrode at different
 478 operating temperature. The platinum reference electrode showed higher potential limit than the
 479 silver wire that was due to the increasing order of reduction potential ($\text{Ag} < \text{Pt}$) in accordance with
 480 electrochemical series. [42]. The reduction potential limit shifts positively by approximately 0.3 V
 481 with an increase in temperature as shown in Fig. 11. This positive shift in reduction potential was

482 due to an increase of temperature that directly influences the electrode kinetics. The recorded
483 reduction potential is illustrated in

484 Table 2. The recorded results clearly show that the reduction potential shifts positively with an
485 increase in the temperature of the eutectic molten hydroxide of approximately 50 °C. The recorded
486 reduction potentials for the reference electrodes used are tabulated in

487 Table 2. The results clearly show a positive shift in the working electrode potential with a molten
488 salt temperature variation of 50 °C for the Ag and Pt electrodes.

489
490 **Table 2.** The reduction potential and current of a 0.5 mm platinum wire working electrode in the eutectic
491 molten hydroxide at various temperatures; with 100 mV s⁻¹ scan rate; CE: 5 mm diameter stainless steel rod;
492 immersion depth: 14 mm; an Ar gas atmosphere: 40 cm³min⁻¹.

Reference electrode	250 °C		300 °C	
	Reduction potential (V)	Current limit (mA)	Reduction potential (V)	Current limit (mA)
Ag wire	-0.99	-0.95	-0.85	-0.52
Pt wire	-1.17	-0.29	-0.87	-0.49
Ni/Ni(OH) ₂ in a mullite tube	-0.63	-117.37	-0.63	-224.50

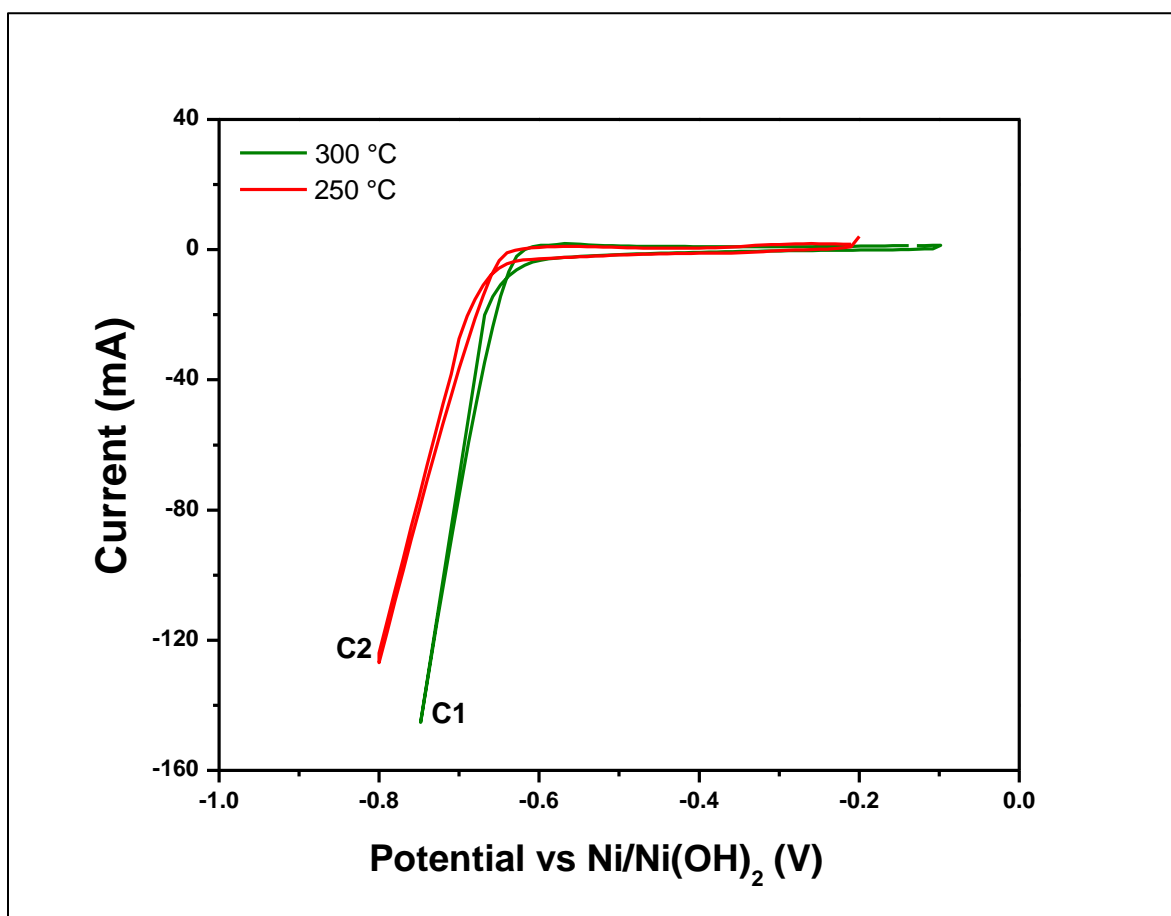
493
494 Using the Ni/Ni(OH)₂ covered with the mullite membrane reference electrode, on the other hand,
495 shows only a slight positive shift in the reduction potential as displayed in Fig. 12 at different
496 operating temperatures and a scan rate of 100 mV s⁻¹. This slight positive shift is due to novel
497 mullite membrane fabrication of Ni/Ni(OH)₂ reference electrode.

498
499

500

501

502



503

504 **Fig. 12.** Cyclic voltammograms of a 0.5 mm Pt wire working electrode in the eutectic molten hydroxide at
505 different temperatures and a scan rate of 100 mV s^{-1} ; CE: 5 mm diameter stainless steel rod; immersion
506 depth: 14 mm; an Ar gas atmosphere: $40 \text{ cm}^3 \text{ min}^{-1}$. RE: Ni/Ni(OH)₂ in a mullite tube.

507

508 The shift in the potential is positive but less than 0.02 V approximately. However, the cathodic

509 limit current increased with an increase in the operating temperature of the eutectic molten

510 hydroxide from -117.37 mA at 250 °C (point C2) to -224.62 mA at 300 °C (point C1). It can be

511 noted here that the increase in the current of the cathodic limit slightly increased with an increase

512 in the operating temperature. This significant increase in the current of cathodic limit is recorded

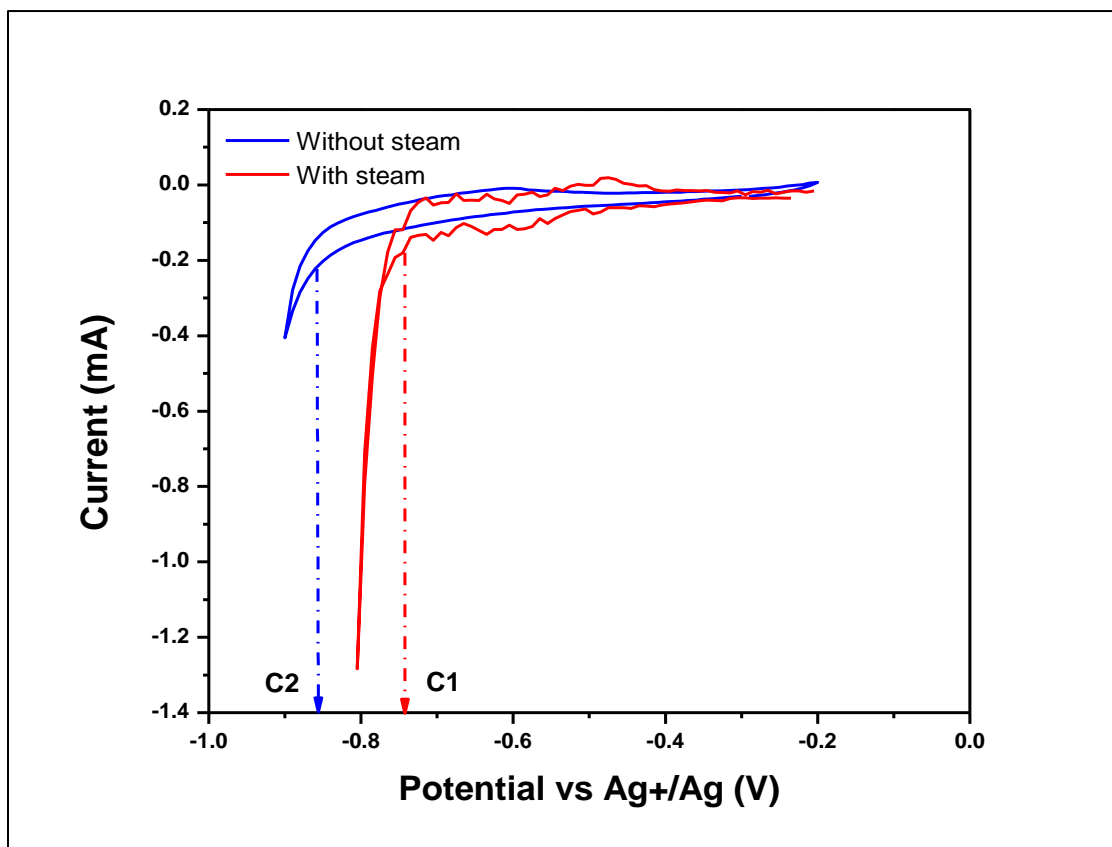
513 in

514 Table 2 and compared with the current of the cathodic limit of other reference electrodes (Ag and
515 Pt). The results of reduction potential and cathodic limit current of Ag, Pt and prepared mullite
516 membrane Ni/Ni(OH)₂ reference electrode that is shown in Fig. 10, Fig. 11 and Fig. 12 highlight
517 the stability of the Ni/Ni(OH)₂ covered with mullite membrane reference electrode in the eutectic
518 molten hydroxide. Because only a slight positive shift of nearly less than 0.02 V is noted in
519 potential which confirms its stability with the rise of temperature as compared to other reference
520 electrodes. This stability and reliability of the nickel reference electrode covered by a mullite
521 membrane tube can be attributed to the eutectic molten hydroxide penetrating through the
522 membrane and reacting with SiO₂. The latter is one of the substances that is used to construct the
523 mullite tube membrane. Consequently, this membrane forms a stable ion channel through it, acting
524 between the internal reference mixture and outside melt. This observed result in terms of stability
525 due to the freshly prepared nickel reference electrode covered by a mullite tube is different from
526 the result obtained from the Ag and Pt reference electrode. The stability of this reference electrode
527 is confirmed and in accordance with the stability analyses of [43]. Miles, Kissel [44] first
528 discovered that increasing the operating temperature of an alkaline electrolysis cell with nickel-
529 based electrodes allowed for increased electrolyte ionic conductivity and enhanced electrode
530 surface kinetics. However, they also found that the main disadvantage of increasing the cell
531 temperature was the reduced durability of cell materials which came into contact with the corrosive
532 electrolyte. Licht et al [1] reported that KOH mixed molten electrolyte affords maximum 800
533 mAcm⁻¹ of current density at less than 1.7 V of electrolysis potential by increasing temperature
534 from 200 to 600 °C. Therefore, the optimum operating temperature of 250 to 300 °C was selected
535 for this study.

536 **3.5 Presence of steam in eutectic molten hydroxide**

537 All the cyclic voltammetry investigations were carried out in the eutectic molten hydroxide under
538 a dry Ar atmosphere. Cyclic voltammetry investigations were hence carried out with the presence
539 of steam to study this effect in the eutectic molten hydroxide on the kinetic activity of the working
540 electrode potential. Firstly, argon gas was bubbled through hot H₂O at 70 °C. Subsequently, argon
541 left the bottle loaded with H₂O. Then, this wet gas stream entered the retort stand which was already
542 at a temperature >225 °C to convert the H₂O in the wet argon to steam. The working electrode used
543 was a platinum wire while the reference electrodes used were Ag and Pt wires, and Ni/Ni(OH)₂
544 covered with a mullite membrane. The molten eutectic hydroxide operating temperature was 225
545 °C and the cyclic voltammetry CV scan rate was 100 mV s⁻¹. Fig. 13 shows the cyclic voltammetry
546 CV of the platinum working electrode obtained with the silver reference electrode with and without
547 the presence of steam.

548



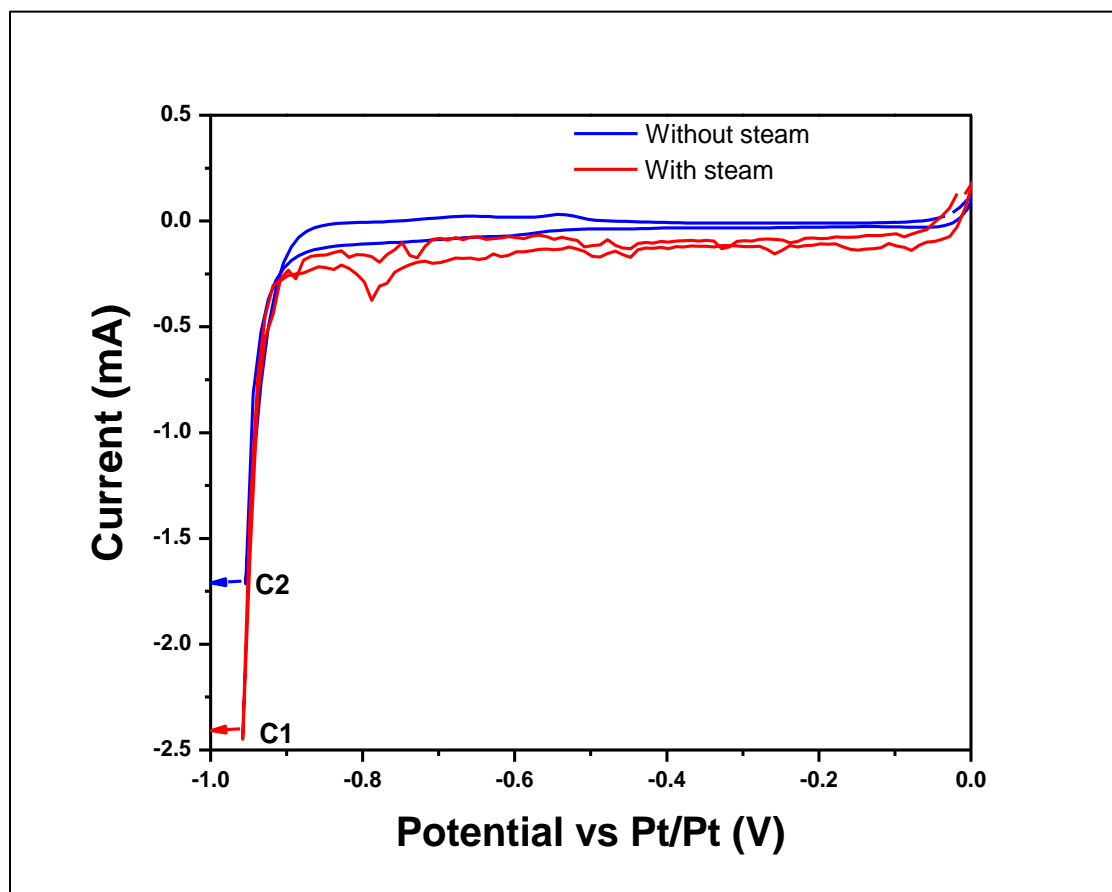
549

550 **Fig. 13.** Cyclic voltammograms of a 0.5 mm Pt wire working electrode in the eutectic molten hydroxide
 551 with and without steam at 225 °C; CE: 5 mm diameter stainless steel rod; RE: 1.0 mm diameter Ag wire;
 552 immersion depth: 14 mm; an Ar gas atmosphere: 40 cm³min⁻¹.
 553

554 It is obvious from Fig. 13 that the cathodic limit shifts positively with the presence of steam inside
 555 the eutectic molten hydroxide. The reduction potential without the presence of steam is -0.88 V
 556 and it shifts positively to -0.75 V with the presence of steam. As can be seen from the figure, a
 557 higher reduction current is also observed with the presence of steam inside the eutectic molten
 558 hydroxide. This rise in reduction current was due to steam that contributes to the electrode
 559 reduction process and enhanced the hydrogen evolution rate at working electrode [27].

560 Table 3 summarises the reduction potential and the current at the cathodic limit achieved with and
 561 without the presence of steam inside the eutectic molten hydroxide. The current at the cathodic
 562 limit increases from -0.41 mA at C2 to -1.26 mA at C1 with the presence of steam. This increase

563 in the current suggests that the presence of steam contributes to the reduction process and hence
564 increases the production rate of hydrogen gas formed at the working electrode (cathode). Fig. 14
565 shows the platinum working electrode cyclic voltammetry with and without steam at the eutectic
566 molten hydroxide operating temperature of 300 °C using platinum wire as the quasi-reference
567 electrode.
568



569
570 **Fig. 14.** Cyclic voltammograms of a 0.5 mm Pt wire working electrode in the eutectic molten hydroxide
571 with and without steam at 300 °C; CE: 5 mm diameter stainless steel rod; RE: 0.5 mm Pt wire; immersion
572 depth: 14 mm; an Ar gas atmosphere: 40 cm³min⁻¹.
573
574 Unlike the silver electrode, the platinum reference electrode showed no obvious difference in the
575 reduction potential with and without the presence of steam inside the eutectic molten hydroxide.

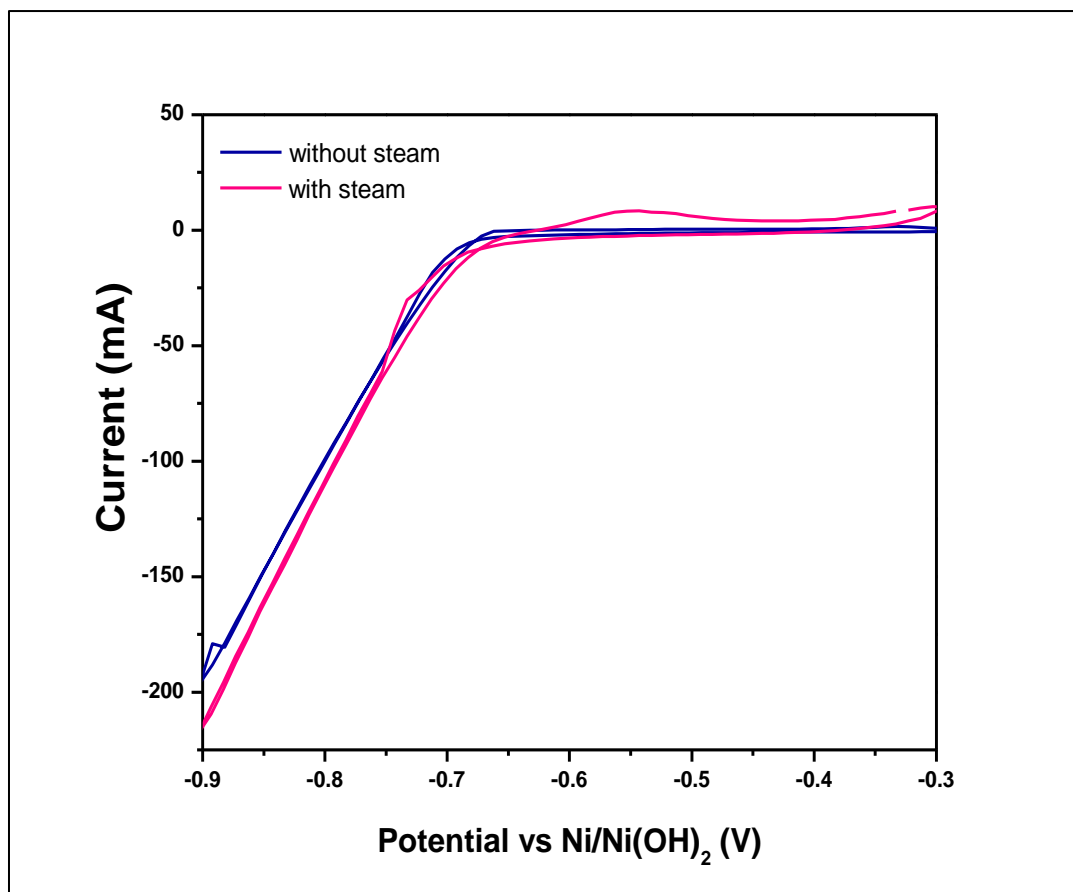
576 In the presence of steam, however, the production rate of hydrogen gas likely increased as noticed
 577 by the increase in current at the cathodic limit C1 (see Fig. 14). In this case, the current increases
 578 from -1.75 mA (without steam at C2) to -2.5 mA (with steam at C1) as reported also in
 579 Table 3. Litch et al., [1] examined a wide range of pure and mixed hydroxide electrolytes such as
 580 LiOH, KOH, NaOH, Ba(OH)₂ and NaOH-KOH at temperatures ranging from 200 to 700 °C. They
 581 also used steam and an argon gas stream inside the electrolyte.

582
 583 **Table 3.** The reduction potential and the current limit produced with and without the presence of steam in
 584 the eutectic molten hydroxide. WE: 0.5 mm Pt wire; CE: 5 mm Stainless steel rod; and RE: 1mm Ag wire at
 585 225 °C, 0.5 mm Pt wire at 300 °C and Ni/Ni(OH)₂ at 225; immersion depth: 14 mm; an Ar gas
 586 atmosphere at 40 cm³min⁻¹.

Reference electrode	Without steam		With steam	
	Reduction potential (V)	Current limit (mA)	Reduction potential (V)	Current limit (mA)
Ag wire	-0.86	-0.41	-0.76	-1.28
Pt wire	-0.88	-1.57	-0.88	-2.45
Ni/Ni(OH) ₂	-0.67	-196.01	-0.66	-217.50

587
 588 Cyclic voltammetry scans using Ni/Ni(OH)₂ reference electrode is displayed in Fig. 15. The
 589 operating temperature during the test was 225 °C, the working electrode was Pt wire and the scan
 590 rate was maintained at 100 mV s⁻¹. The electrochemical behaviour of the working electrode was
 591 the same with and without presence steam as shown in Fig. 15. The reduction potential of prepared
 592 nickel electrode for hydrogen gas formation is still the same at -0.67 V with and without steam.
 593 Therefore, the platinum working electrode controlled by the prepared Ni/Ni(OH)₂ reference
 594 electrode produces stable cyclic voltammetry results even when water is found in the eutectic
 595 molten hydroxide.

596



597
 598 **Fig. 15.** Cyclic voltammograms of a 0.5 mm Pt wire working electrode in the eutectic molten hydroxide
 599 with and without steam at an operating temperature of 225 °C and a scan rate of 100 mV s⁻¹; CE: 5mm
 600 diameter stainless steel rod; RE: Ni/Ni(OH)₂ in a mullite tube; Immersion Depth: 14 mm; an Ar gas
 601 atmosphere:40 cm³min⁻¹.
 602
 603 In general, the presence of steam inside the eutectic molten hydroxide increases slightly the value
 604 of the cathodic limit current implying an increase in the yield of hydrogen gas. This stable reduction
 605 potential behaviour is also similar to that obtained using the platinum reference electrode. In terms
 606 of gas produced, however, the cathodic current obtained when the Pt reference electrode was used
 607 is only -2.5 mA while that for the Ni/Ni(OH)₂ electrode is -217.3 mA. This observed current
 608 indicates that the latter has a higher evolution of the hydrogen gas reaction than without the
 609 presence of steam [27]. In other words, the Ni/Ni(OH)₂ covered with a mullite membrane reference

610 electrode designed in this research has proven to be very stable in effectively controlling the
611 potential of the Platinum working electrode. This leads to a high cathodic product (hydrogen gas).

612 **4. Conclusions**

613 A new reference electrode for eutectic molten hydroxide was fabricated by covering Ni/Ni(OH)₂
614 with an ionic membrane of mullite tube. The prepared reference electrode was compared with silver
615 and platinum quasi-reference electrodes in the same operating conditions. The findings of this
616 work can be summarised as follows:

- 617 • Eutectic molten hydroxide (NaOH-KOH; 49–51 mol%) at 225 °C is -1.96 V and this was
618 calculated using HSC chemistry software (version 6.1; outotec).
- 619 • The cyclic voltammetry investigation shows that when the potential scan rate was changed,
620 the current limit changed and this change in current confirmed that mass transport can occur
621 under semi-infinite linear diffusion conditions at the cathodic limit of the platinum working
622 electrode.
- 623 • One of the more significant findings to emerge from this study is that increasing the
624 operating temperature of molten hydroxides by about 50°C shifted the reduction potential
625 of both silver and platinum reference electrodes. However, only a slight positive shift of
626 0.02 V was observed with prepared Ni/Ni(OH)₂ covered with a mullite membrane that
627 suggests it has good stability as temperature varies.
- 628 • The results also indicate that the prepared nickel and platinum reference electrode can be
629 used to control the platinum working electrode, thereby producing stable and reliable cyclic
630 voltammetry results with and without the presence of steam in the eutectic molten

631 hydroxide. The silver reference electrode, on the other hand, showed positive shifts of up
632 to 0.1V in the reduction potential.

633 • From above results, it can be concluded that the Ni/Ni(OH)₂ covered with a mullite
634 membrane reference electrode compared with Ag and Pt reference electrode has shown to
635 be very stable in effectively controlling the potential of the Platinum working electrode.
636 This subsequently leads to a high cathodic product yield (hydrogen gas). Therefore,
637 effective control of the working electrode by the stable reference electrode directly
638 contributes to increasing the hydrogen gas evolution reaction through constructing a stable
639 ion channel.

640 **References**

- 641 1. Licht, S., et al., Comparison of alternative molten electrolytes for water splitting to generate
642 hydrogen fuel. *Journal of The Electrochemical Society*, 2016. 163(10): p. F1162-F1168.
- 643 2. Guo, L., et al., Development of a low temperature, molten hydroxide direct carbon fuel cell.
644 *Energy & Fuels*, 2013. 27(3): p. 1712-1719.
- 645 3. Lu, Y., et al., Electrodeposition of NiMoCu coatings from roasted nickel matte in deep
646 eutectic solvent for hydrogen evolution reaction. *International Journal of Hydrogen Energy*,
647 2019. 44(12): p. 5704-5716.
- 648 4. Chen, L., et al., Separating hydrogen and oxygen evolution in alkaline water electrolysis
649 using nickel hydroxide. *Nature communications*, 2016. 7: p. 11741.
- 650 5. Santos, D.M., C.A. Sequeira, and J.L. Figueiredo, Hydrogen Production by Alkaline Water
651 Electrolysis. *Química Nova*, 2013. 36(8): p. 1176-1193.
- 652 6. Gupta, R.B., Hydrogen fuel: production, transport, and storage. 2008: Crc Press.
- 653 7. Hosseini, S.E. and M.A. Wahid, Hydrogen production from renewable and sustainable
654 energy resources: promising green energy carrier for clean development. *Renewable and
655 Sustainable Energy Reviews*, 2016. 57: p. 850-866.
- 656 8. Vivas, F., et al., A review of energy management strategies for renewable hybrid energy
657 systems with hydrogen backup. *Renewable and Sustainable Energy Reviews*, 2018. 82: p.
658 126-155.
- 659 9. Cipriani, G., et al., Perspective on hydrogen energy carrier and its automotive applications.
660 *International Journal of Hydrogen Energy*, 2014. 39(16): p. 8482-8494.
- 661 10. Alam, H.B., et al., Surface characteristics and electrolysis efficiency of a Palladium-Nickel
662 electrode. *international journal of hydrogen energy*, 2018. 43(4): p. 1998-2008.
- 663 11. Sharma, S. and S.K. Ghoshal, Hydrogen the future transportation fuel: from production to
664 applications. *Renewable and sustainable energy reviews*, 2015. 43: p. 1151-1158.
- 665 12. Dincer, I. and C. Acar, Review and evaluation of hydrogen production methods for better
666 sustainability. *International journal of hydrogen energy*, 2015. 40(34): p. 11094-11111.
- 667 13. Maric, R. and H. Yu, Proton Exchange Membrane Water Electrolysis as a Promising
668 Technology for Hydrogen Production and Energy Storage, in *Nanostructures in Energy
669 Generation, Transmission and Storage*. 2018, IntechOpen.
- 670 14. Papaderakis, A., et al., Hydrogen evolution at Ir-Ni bimetallic deposits prepared by galvanic
671 replacement. *Journal of Electroanalytical Chemistry*, 2018. 808: p. 21-27.
- 672 15. Ursua, A., L.M. Gandia, and P. Sanchis, Hydrogen Production From Water Electrolysis:
673 Current Status and Future Trends. *Proceedings of the IEEE*, 2012. 100(2): p. 410-426.
- 674 16. Zeng, K. and D. Zhang, Recent Progress in Alkaline Water Electrolysis for Hydrogen
675 Production and Applications. *Progress in Energy and Combustion Science*, 2010. 36(3): p.
676 307-326.
- 677 17. Mazloomi, S. and N. Sulaiman, Influencing factors of water electrolysis electrical
678 efficiency. *Renewable and Sustainable Energy Reviews*, 2012. 16(6): p. 4257-4263.

- 679 18. Miles, M., Exploration of molten hydroxide electrochemistry for thermal battery
680 applications. *Journal of applied electrochemistry*, 2003. 33(11): p. 1011-1016.
- 681 19. Ge, J., et al., Metallic nickel preparation by electro-deoxidation in molten sodium
682 hydroxide. *Journal of The Electrochemical Society*, 2015. 162(9): p. E185-E189.
- 683 20. Liu, T., et al., Self-Standing CoP Nanosheets Array: A Three-Dimensional Bifunctional
684 Catalyst Electrode for Overall Water Splitting in both Neutral and Alkaline Media.
685 *ChemElectroChem*, 2017. 4(8): p. 1840-1845.
- 686 21. Gong, Y., et al., Synthesis of defect-rich palladium-tin alloy nanochain networks for formic
687 acid oxidation. *Journal of colloid and interface science*, 2018. 530: p. 189-195.
- 688 22. Zhang, Z., et al., Facile fabrication of stable PdCu clusters uniformly decorated on graphene
689 as an efficient electrocatalyst for formic acid oxidation. *International Journal of Hydrogen
690 Energy*, 2019. 44(5): p. 2731-2740.
- 691 23. Zhang, L.Y., et al., Palladium-cobalt nanodots anchored on graphene: In-situ synthesis, and
692 application as an anode catalyst for direct formic acid fuel cells. *Applied Surface Science*,
693 2019. 469: p. 305-311.
- 694 24. Wu, D., et al., γ -Fe₂O₃ nanoparticles stabilized by holey reduced graphene oxide as a
695 composite anode for lithium-ion batteries. *Journal of colloid and interface science*, 2019.
696 552: p. 633-638.
- 697 25. Zhu, W., et al., Design and application of foams for electrocatalysis. *ChemCatChem*, 2017.
698 9(10): p. 1721-1743.
- 699 26. Yang, J., et al., Development of a direct ammonia-fueled molten hydroxide fuel cell.
700 *Journal of Power Sources*, 2014. 245: p. 277-282.
- 701 27. Licht, S., et al., Ammonia synthesis by N₂ and steam electrolysis in molten hydroxide
702 suspensions of nanoscale Fe₂O₃. *Science*, 2014. 345(6197): p. 637-640.
- 703 28. Hrnčiarikova, L., et al., The influence of anode composition on the electrochemical ferrate
704 (VI) production in molten KOH. *Int J Electrochem Sci*, 2013. 8(6): p. 7768-7778.
- 705 29. Híveš, J., et al., Electrochemical formation of ferrate (VI) in a molten NaOH–KOH system.
706 *Electrochemistry communications*, 2006. 8(11): p. 1737-1740.
- 707 30. Schiavon, G., S. Zecchin, and G.G. Bombi, Copper (I)-Copper Reference Electrode in
708 Molten Hydroxides. *Journal of Electroanalytical Chemistry and Interfacial
709 Electrochemistry*, 1972. 38(2): p. 473-475.
- 710 31. Zaafarany, I. and H. Boller, Electrochemical Behavior of Copper Electrode in Sodium
711 Hydroxide Solutions. *Current World Environment*, 2009. 4(2): p. 277-284.
- 712 32. Xie, L., et al., In situ formation of a 3D core/shell structured Ni₃N@Ni–Bi nanosheet
713 array: an efficient non-noble-metal bifunctional electrocatalyst toward full water splitting
714 under near-neutral conditions. *Journal of Materials Chemistry A*, 2017. 5(17): p. 7806-
715 7810.
- 716 33. Döner, A., İ. Karcı, and G. Kardaş, Effect of C-felt supported Ni, Co and NiCo catalysts to
717 produce hydrogen. *International Journal of Hydrogen Energy*, 2012. 37(12): p. 9470-9476.

- 718 34. Pal, R., et al., Development and Electrochemistry of a Novel Ag/AgCl Reference Electrode
719 Suitable for Mixed Chloride–fluoride Melts. *Electrochimica Acta*, 2011. 56(11): p. 4276-
720 4280.
- 721 35. Martin, A., et al., Yttria-Stabilized Zirconia as Membrane Material for Electrolytic
722 Deoxidation of CaO–CaCl₂ Melts. *Journal of applied electrochemistry*, 2010. 40(3): p. 533-
723 542.
- 724 36. Wang, H., et al., A robust alumina membrane reference electrode for high temperature
725 molten salts. *Journal of The Electrochemical Society*, 2012. 159(9): p. H740-H746.
- 726 37. Gayer, K.H. and A. Garrett, The Equilibria of Nickel Hydroxide, Ni (OH)₂, in Solutions of
727 Hydrochloric Acid and Sodium Hydroxide at 25^oC. *Journal of the American Chemical*
728 *Society*, 1949. 71(9): p. 2973-2975.
- 729 38. Zoulias, E., et al., A review on Water Electrolysis. *TCJST*, 2004. 4(2): p. 41-71.
- 730 39. Kovendhan, M., et al., Alternative cost-effective electrodes for hydrogen production in
731 saline water condition. *International Journal of Hydrogen Energy*, 2019. 44(11): p. 5090-
732 5098.
- 733 40. Liu, Q., et al., A porous Ni₃N nanosheet array as a high-performance non-noble-metal
734 catalyst for urea-assisted electrochemical hydrogen production. *Inorganic Chemistry*
735 *Frontiers*, 2017. 4(7): p. 1120-1124.
- 736 41. Cao, X., et al., One-step co-electrodeposition of hierarchical radial Ni₉P nanospheres on
737 Ni foam as highly active flexible electrodes for hydrogen evolution reaction and
738 supercapacitor. *Chemical Engineering Journal*, 2018. 348: p. 310-318.
- 739 42. Rong, K., et al., Electrochemical fabrication of nanoporous gold electrodes in a deep
740 eutectic solvent for electrochemical detections. *Chemical Communications*, 2018. 54(64):
741 p. 8853-8856.
- 742 43. Fu, G., et al., Highly conductive solid polymer electrolyte membranes based on
743 polyethylene glycol-bis-carbamate dimethacrylate networks. *Journal of Power Sources*,
744 2017. 359: p. 441-449.
- 745 44. Miles, M., et al., Effect of Temperature on Electrode Kinetic Parameters for Hydrogen and
746 Oxygen Evolution Reactions on Nickel Electrodes in Alkaline Solutions. *Journal of the*
747 *Electrochemical Society*, 1976. 123(3): p. 332-336.
748